

## **Chapter 3.**

# **The Regulation of Noise in a Metabolic Gene Determines an Ecological Strategy in Yeast**

Parts reproduced from:

Travis S. Bayer, Kevin G. Hoff, Chase L. Beisel, Jack J. Lee, and Christina D. Smolke, **The regulation of noise in a metabolic gene determines an ecological strategy in yeast**, In review.

Evolutionary theory suggests that genetic regulatory circuits optimize protein expression levels to maximize fitness.<sup>1,2</sup> However, the dependence of fitness on levels of a regulator protein across varying environmental conditions has seldom been measured. Here, we found that varying the expression of a transcriptional regulator of nitrogen metabolism, Dal80p<sup>3</sup>, mediates a trade-off in fitness between resource-abundant and resource-limiting environments in *Saccharomyces cerevisiae* by modulating noise in the expression of a nitrogen metabolic enzyme, glutamate dehydrogenase (Gdh1p). Redundancy in the metabolic pathways and the regulatory network structure of ammonia assimilation allowed noise rather than abundance of Gdh1p to determine a classic dichotomy in ecological strategies: whether to specialize in maximizing fitness in resource abundant (rate strategy), or to specialize in maximizing fitness in resource limiting environments (yield strategy).<sup>4,5</sup> Our results suggest that the optimization of protein noise may be as important as the optimization of protein expression levels for crafting ecological strategies to environmental demands.

The ability to assimilate and utilize nitrogen is a significant component of fitness in *S. cerevisiae*, and yeast display considerable strain-to-strain variation in the utilization of this key resource.<sup>6</sup> Nitrogen metabolism is largely controlled by a complex network of auto- and cross-regulation of four transcriptional regulators: Gln3p, Gat1p, Gzf3p, and Dal80p<sup>7</sup> (**Fig. 1**). We replaced the endogenous promoter of *DAL80* with the *GAL1-10* promoter by chromosomal integration (**Fig. 2a**) to achieve galactose-tunable control<sup>8</sup> of Dal80p (**Fig. 2b**). We then measured fitness of the  $P_{GAL-DAL80}$  strain at various Dal80p levels across a range of ammonia concentrations (spanning near growth limiting to near toxic conditions)<sup>9</sup> by direct competition with a reference strain.<sup>10</sup> At low expression of Dal80p, the engineered strain displayed lower fitness than the parent strain at low ammonia concentrations, and higher fitness with increasing ammonia concentrations (**Fig. 3a**). Conversely, high Dal80p expression led to high relative fitness of the engineered strain at low ammonia and progressively lower fitness as ammonia concentration increased. To parameterize the fitness effects, we defined an environment-dependent fitness term,  $W_{env}$ , as the ratio of fitness in high ammonia (556 mM) to fitness in low ammonia (8.6 mM).  $W_{env}$  values greater than 1 indicate strains that are more competitive at high ammonia, where values less than 1 indicate strains more competitive at low ammonia (**Fig. 3b**).

Depending on the level of Dal80p expression, strains are either superior competitors in high or low ammonia concentrations, demonstrating a trade-off in fitness across environments. This fitness trade-off is specific to ammonia as a nitrogen source (**Fig. 4a**) and is dependent on all three ammonia assimilation pathways (**Fig. 4b**). Trade-offs have been demonstrated between traits such as reproduction and growth, longevity

and fecundity, and competitive ability and resistance to invasion.<sup>11-13</sup> One of the most prominent trade-off theories in biology is that of  $r$  versus  $K$  strategists.<sup>4</sup> Organisms displaying a  $K$  strategy are predicted to optimize utilization of resources, such as when the population is near its carrying capacity and resources are scarce, while  $r$  strategists are predicted to dominate when resources are abundant. These trade-offs are often underpinned by trade-offs in cellular biochemistry such as rate and yield of enzymatic reactions<sup>14</sup> and substrate uptake and affinity of resource transport.<sup>15</sup> We next examined the effect of changing Dal80p levels on the primary route of ammonia assimilation in yeast, glutamate dehydrogenase (Gdh1p). Analysis of single-cell expression of a Gdh1p:GFP fusion protein via flow cytometry in the  $P_{GAL}$ -*DAL80* strain revealed that increasing levels of Dal80p had little effect on mean Gdh1p abundance (**Fig. 5a**), but changed the noise in Gdh1p expression. Noise, or stochastic fluctuations in the abundance of proteins, can be enhanced or attenuated by regulatory circuits<sup>16</sup> and has been shown to be critical in biological functions such as determining viral latency<sup>17</sup> and competence in *Bacillus subtilis*.<sup>18</sup> In our engineered strain, low levels of Dal80p resulted in higher noise in Gdh1p expression (15% higher than the parent), while high levels of Dal80p reduced noise relative to the parent strain (20% lower than the parent) (**Fig. 5c**). Mean Gdh1p abundances remained relatively constant across all Dal80p levels (**Fig. 5d**).

To test whether noise in Gdh1p expression was correlated with the observed fitness trends independently of other Dal80p targets or galactose inducer effects, we generated a set of mutants with varying Gdh1p abundance and noise values by mutating the *GDH1* promoter. We identified sets of mutants having similar abundances and variable noise in Gdh1p expression (**Fig. 6a**), such that the contribution of either noise or

abundance could be parsed. We measured  $W_{\text{env}}$  in these mutant sets and observed a stronger positive correlation with noise in Gdh1p expression (correlation coefficient = 0.83,  $R^2 = 0.69$ ) than abundance (correlation coefficient = 0.079,  $R^2 = 0.0062$ ) (**Fig. 6b**).

To examine whether stochastic fluctuations in the expression of an enzyme can affect the total rate of product formation, we used the Gillespie algorithm to perform a stochastic simulation of the expression of an enzyme that converts a substrate into a single product (**Fig. 7a**). The simulation results show a classic hyperbolic enzyme titration curve (**Fig. 7b**). To examine the effect of noise on this system, we repeated the simulations, keeping the mean abundance of the enzyme constant while varying noise in enzyme expression (**Fig. 8a**). We then performed a series of simulations for different enzyme abundance values and calculated the noise dependence of the effective rate for each mean enzyme value (**Fig. 8b**). Noise dependence passes through a maximum value in these simulations, corresponding to the “cusp” of the enzyme titration plateau (**Fig. 7b**), indicating that there is a region of enzyme abundance where the system is most susceptible to noise. One qualitative prediction of this simulation is that noise will have a lower impact on product formation rates at high enzyme levels.

The above simulations and data suggest that noisy enzyme expression can decrease the rate of product formation from Gdh1p. Thus, a strain with lower rates of Gdh1p catalysis should show similar fitness trends as a high noise strain, whereas a strain with higher rates of Gdh1p catalysis should show fitness trends similar to a low noise strain. To test this, we replaced the endogenous copy of Gdh1p with previously characterized Gdh1p rate-enhanced and rate-deficient mutants. The D150H mutant was shown to have a 1000-fold lower rate measured *in vitro*, while the C313S mutant showed

a 0.4-fold increase in rate.<sup>19</sup> The catalytic rate-deficient D150H mutant was more competitive than the parent strain in high concentrations of ammonia ( $\text{NH}_4^+ > 278 \text{ mM}$ ) and was lower fitness than the parent strain in low ammonia concentrations (**Fig. 9**). In contrast, the catalytic rate-enhanced C313S mutant was less fit than the parent strain in high ammonia environments and displayed higher fitness in low ammonia concentrations.

Taken together, the simulations and data suggest that Gdh1p rates are correlated with fitness in different ways in high and low ammonia environments. For example, at low ammonia concentrations, fitness is positively correlated with Gdh1p rate: the catalytic mutant with high rate showed higher fitness as observed with strains with low noise, which confers higher effective rates according to simulations. A positive correlation of metabolic pathway rates with growth rate has been highlighted in ATP synthesis in microbes.<sup>20</sup> Conversely, in rich ammonia environments, Gdh1p rate is negatively correlated with fitness: the catalytic mutant with high rate showed low fitness, whereas the mutant with lower catalytic rate showed higher fitness. We speculate that the accumulation of downstream metabolites may have deleterious effects on fitness, as has been observed in the perturbation of AdoMet synthesis and methionine hyperaccumulation in yeast.<sup>21</sup>

Regardless of the mechanism through which Gdh1p rate affects fitness, the catalytic point mutants show that the rate of Gdh1p catalysis can impact fitness in different ammonia environments, while the simulations demonstrate how noise can affect the effective rate of reaction, drawing a causal link between Gdh1p noise and fitness trends. However, one would also expect changes in mean Gdh1p abundance to affect effective catalytic rates. Yeast possess an alternate route through which to synthesize

glutamate from ammonia, the NAD-dependent glutamate synthase Glt1p<sup>22</sup>. Glt1p has been shown to be upregulated 3-fold in Gdh1p deletion strains,<sup>22</sup> and titration studies with Dal80p and Gdh1p indicate that *GLT1* transcript levels are inversely correlated with Gdh1p abundance but not noise (**Figs. 10a,b**). These results indicate that regulatory networks controlling levels of Glt1p may provide a mechanism to buffer large-scale changes in Gdh1p expression. Deletion of *GLT1* may remove this “balancing” and impact how  $W_{\text{env}}$  trends correlate with Gdh1p abundance and noise.

We measured the relationship between noise, abundance, and  $W_{\text{env}}$  in the absence of this redundant pathway by constructing a *GDH1* promoter library (as before) in a *GLT1Δ* background strain. For these mutants,  $W_{\text{env}}$  shows stronger negative correlation with Gdh1p abundance (**Fig. 11a**, correlation coefficient = -0.41,  $R^2 = 0.48$ ), than Gdh1p noise (**Fig. 11b**, correlation coefficient = 0.02,  $R^2 = 10^{-5}$ ). These trends are in contrast to those observed previously (**Fig. 6b**) and to a similar experiment with wildtype *GLT1* (**Fig. 12a**,  $W_{\text{env}}$  versus noise: correlation coefficient = 0.52,  $R^2 = 0.27$ ; **Fig. 12b**,  $W_{\text{env}}$  versus abundance: correlation coefficient = 0.19,  $R^2 = 0.03$ ). In the *GLT1Δ* background, mutants with low Gdh1p levels show high  $W_{\text{env}}$  values, as would be expected from canonical enzyme titration (less enzyme results in lower product formation rates, showing similar fitness trends to the rate-deficient D150H mutant). The presence or absence of Glt1p, an alternate route for ammonia assimilation, determines whether noise (in the presence of Glt1p) or abundance (in the absence of Glt1p) of Gdh1p determines phenotypic behavior in a sampling of mutants (**Fig. 13**). As an additional control for this model, we overexpressed Glt1p in a set of *GDH1* promoter mutants. Increasing the amount of this enzyme should push the system into a regime where rates (and, therefore,

fitness) are not as sensitive to Gdh1p noise, according to the above simulation. We found that *GLT1* overexpression diminished the effect Gdh1p noise had on  $W_{env}$  (**Fig. 14**), supporting that wildtype Gdh1p and Glt1p abundances are in a regime where fitness is susceptible to noise.

Because noise in Gdh1p expression determines an ecological strategy, then environmental conditions should select for members of a population showing high or low noise depending on the favored strategy. To test this hypothesis, we competed the *GDHI* promoter library in two batch culture ammonia environments (139 mM and 556 mM) to impose different selection pressures. Here, higher ammonia is predicted to have stronger selection pressure for rate strategists.<sup>5</sup> After 36 generations of competition, a sampling of individuals from each environment revealed populations that were largely clustered around the noise and  $W_{env}$  values of the initial library (**Fig. 15a, b**). At 60 generations, both populations show enrichment for rate strategists ( $W_{env} > 1$ ) versus the initial library (**Fig. 15c**). Interestingly, each population is composed of a mixture of rate and yield strategists. Importantly, the 556 mM environment enriched for mutants with higher average noise in Gdh1p expression than the parent strain ( $CV^2_{initial} = 0.61$ ,  $CV^2_{evolved} = 0.65$ ,  $P = 0.007$ ), as well as rate strategists ( $W_{env, initial} = 0.91$ ,  $W_{env, evolved} = 1.69$ ,  $P = 0.01$ ). The 139 mM environment enriched for mutants displaying lower noise than the parent strain ( $CV^2_{initial} = 0.61$ ,  $CV^2_{evolved} = 0.56$ ,  $P = 1.5 \times 10^{-6}$ ). No such enrichment was observed when comparing mean Gdh1p abundance from each evolved population (**Fig. 16**,  $p_{139mM} = 0.85$ ,  $p_{556mM} = 0.86$ ,  $P = 0.72$ ). Thus, because noise in Gdh1p expression is linked with the *r* and *K* phenotypes, it can be shaped by environments that select for those

phenotypes. To our knowledge, this is the first demonstration that gene expression noise is a selectable trait.

One of the more concrete definitions of  $r$  and  $K$  strategies is the notion of density-dependent selection:  $r$  strategists show fitness advantage at low population density, while  $K$  strategists show advantage at high density. To test if strains differing only in Gdh1p noise displayed this behavior, we designated two clones that displayed high and low noise values from the evolved populations (at 60 generations) but similar abundance values as  $r$  and  $K$ , respectively (**Fig. 17a**). We then competed these strains versus a reference strain as above at varying initial densities for 24 hours to simulate a “season” of competition.<sup>23</sup> Competitions were performed in the lowest (8.6 mM) and highest (556 mM) ammonia concentrations measured to simulate a resource-poor and resource-abundant environment, respectively. The fitness of the high noise  $r$  strategist is negative density-dependent, implying that this strain is a better competitor in low-density environments (**Fig. 17b**). The density-dependence in the high ammonia environment is not as severe, suggesting that the abundance of ammonia determines how stringent competition will be for a given population density. Conversely, the  $K$  strategist is more competitive than the  $r$  strain at high population densities, demonstrating that strains differing in Gdh1p expression noise can recapitulate canonical ecological strategies.<sup>24</sup>

By measuring an environment-dependent fitness as a function of a regulator level, we were able to uncover a  $r/K$  trade-off in ammonia metabolism that is modulated by noise in the expression of a metabolic gene, *GDH1*, and not mean abundance of this enzyme by virtue of cross-regulation with a redundant pathway. The expression of Dal80p itself is known to be sensitive to nitrogen catabolite repression (NCR), where

expression is upregulated in nitrogen starvation, environments with non-preferred nitrogen sources, or addition of the small molecule rapamycin.<sup>3</sup> The strategy of Gdh1p noise regulation in varying nitrogen environments is an interesting topic for future study in that strains that differed only in Gdh1p expression noise showed canonical  $r$  and  $K$  density-dependent behavior, indicating that noise is able to shape an ecological strategy in nitrogen assimilation. The results presented here may be relevant to other metabolic pathways and organisms, as metabolic redundancy is widespread throughout Nature. While it may be advantageous to harbor duplicate and/or redundant genes and pathways to buffer the effects of gene loss, redundant pathways may also present additional opportunities for the regulation of metabolism and fitness. Regulatory mechanisms that buffer noise in gene expression, such as negative feedback, may be indicative of ancestral adaptation towards specific environments. An exploration of the network architectures regulating such systems will reveal whether the emergence of alternative routes for metabolic processes has presented evolution with a design opportunity for modulating ecological strategy. Taken together, these results illustrate that regulatory networks may optimize noise in gene expression in addition to protein levels to fashion adaptive solutions to environmental challenges, and suggest a link between networks of genetic regulation and networks of ecological interactions.

### **Methods Summary**

**Strains and media.** All manipulations were performed with derivatives of the S288c background from the University of California San Francisco GFP-tag collection

(Invitrogen).<sup>25</sup> Yeast were grown in synthetic complete media (1.7 g/L yeast nitrogen base, nitrogen source as specified).

**Competitions and fitness assays.** Fitness was assayed by direct competition versus a common reference strain<sup>10</sup>. The competitor and reference strain constitutively express different fluorescent proteins (GFP and CFP, respectively) from the *ADHI* promoter integrated into the chromosome. The frequency of competitor and reference strain were quantitated before and after the growth period by counting the numbers of GFP expressing cells to non-GFP expressing cells. Fitness ( $w$ ) of the competitor strain is reported as the natural log of the change in frequency of the strain versus the reference strain during the competitive growth period over the change in frequency of the parent strain versus the reference strain over the same growth period:

$$w = \ln \left( \frac{\text{fold change of the engineered strain after competition with reference strain}}{\text{fold change of the parent strain after competition with reference strain}} \right)$$

**Calculation of noise.** Noise was calculated as the square of the coefficient of variation of the distribution<sup>26</sup>.

**Mutagenic PCR and construction of promoter libraries.** A construct comprising the region approximately 500 nucleotides upstream of the *GDHI* coding region was subjected to error-prone PCR, assembled with a selectable marker, and transformed into the specified strain background.

**Gillespie simulations.** Simulations were performed as previously described,<sup>27</sup> with the probability of reaction occurring in a given time interval proportional to the reaction rate. Noise was introduced by varying the ratio of mRNA decay rate to protein synthesis rate

(burst size of protein production). Compensatory changes in mRNA synthesis rate were adjusted to simulate expression with varying noise and similar abundance.

**Experimental evolution.** Aliquots from the *GDH1* promoter library were diluted into 2 mL synthetic complete with either 139 mM ammonia or 556 mM ammonia. Populations were grown in batch culture and diluted 10<sup>3</sup>-fold into respective fresh media every 24 hours.

**Statistical analysis.** Pearson correlation coefficients were calculated with either Gdh1p noise or abundance as the dependent variable and  $W_{env}$  as the independent variable, respectively. Significance of population averaged  $W_{env}$  and noise values in evolution experiments was calculated with a two-tailed t-test. Data was tested for normality using the Kolmogorov-Smirnov test. The mean  $\pm$ s.d. from at least three independent experiments is shown for all data.

**Detailed methods can be found in Appendix B.**

## References

1. Rosen, R. Optimality principles in biology (Butterworths, London,, 1967).
2. Orr, H. A. The genetic theory of adaptation: a brief history. *Nat Rev Genet* 6, 119-27 (2005).
3. Cunningham, T. S., Rai, R. & Cooper, T. G. The level of DAL80 expression down-regulates GATA factor-mediated transcription in *Saccharomyces cerevisiae*. *J Bacteriol* 182, 6584-91 (2000).
4. MacArthur, R. H. & Wilson, E. O. The theory of island biogeography (Princeton University Press, Princeton, N.J.,, 1967).
5. Pianka, E. R. R-Selection and K-Selection. *American Naturalist* 104, 592-& (1970).
6. Homann, O. R., Cai, H., Becker, J. M. & Lindquist, S. L. Harnessing natural diversity to probe metabolic pathways. *PLoS Genet* 1, e80 (2005).

7. Cooper, T. G. Transmitting the signal of excess nitrogen in *Saccharomyces cerevisiae* from the Tor proteins to the GATA factors: connecting the dots. *FEMS Microbiol Rev* 26, 223-38 (2002).
8. Hawkins, K. M. & Smolke, C. D. The regulatory roles of the galactose permease and kinase in the induction response of the GAL network in *Saccharomyces cerevisiae*. *J Biol Chem* 281, 13485-92 (2006).
9. Hess, D. C., Lu, W., Rabinowitz, J. D. & Botstein, D. Ammonium toxicity and potassium limitation in yeast. *PLoS Biol* 4, e351 (2006).
10. Elena, S. F. & Lenski, R. E. Evolution experiments with microorganisms: the dynamics and genetic bases of adaptation. *Nat Rev Genet* 4, 457-69 (2003).
11. Ghalambor, C. K., Reznick, D. N. & Walker, J. A. Constraints on adaptive evolution: the functional trade-off between reproduction and fast-start swimming performance in the Trinidadian guppy (*Poecilia reticulata*). *Am Nat* 164, 38-50 (2004).
12. Rose, M. & Charlesworth, B. A test of evolutionary theories of senescence. *Nature* 287, 141-2 (1980).
13. Weitz, J. S., Hartman, H. & Levin, S. A. Coevolutionary arms races between bacteria and bacteriophage. *Proc Natl Acad Sci U S A* 102, 9535-40 (2005).
14. Pfeiffer, T., Schuster, S. & Bonhoeffer, S. Cooperation and competition in the evolution of ATP-producing pathways. *Science* 292, 504-7 (2001).
15. Gudelj, I., Beardmore, R. E., Arkin, S. S. & MacLean, R. C. Constraints on microbial metabolism drive evolutionary diversification in homogeneous environments. *J Evol Biol* 20, 1882-9 (2007).
16. Rao, C. V., Wolf, D. M. & Arkin, A. P. Control, exploitation and tolerance of intracellular noise. *Nature* 420, 231-7 (2002).
17. Weinberger, L. S., Burnett, J. C., Toettcher, J. E., Arkin, A. P. & Schaffer, D. V. Stochastic gene expression in a lentiviral positive-feedback loop: HIV-1 Tat fluctuations drive phenotypic diversity. *Cell* 122, 169-82 (2005).
18. Suel, G. M., Garcia-Ojalvo, J., Liberman, L. M. & Elowitz, M. B. An excitable gene regulatory circuit induces transient cellular differentiation. *Nature* 440, 545-50 (2006).
19. Wang, X. G. & Engel, P. C. Identification of the reactive cysteine in clostridial glutamate dehydrogenase by site-directed mutagenesis and proof that this residue is not strictly essential. *Protein Eng* 7, 1013-6 (1994).
20. Pfeiffer, T. & Bonhoeffer, S. Evolution of cross-feeding in microbial populations. *Am Nat* 163, E126-35 (2004).
21. Lu, P. et al. Global metabolic changes following loss of a feedback loop reveal dynamic steady states of the yeast metabolome. *Metab Eng* 9, 8-20 (2007).
22. Valenzuela, L., Ballario, P., Aranda, C., Filetici, P. & Gonzalez, A. Regulation of expression of GLT1, the gene encoding glutamate synthase in *Saccharomyces cerevisiae*. *J Bacteriol* 180, 3533-40 (1998).
23. MacLean, R. C. & Gudelj, I. Resource competition and social conflict in experimental populations of yeast. *Nature* 441, 498-501 (2006).
24. Sutherland, W. J. *From individual behaviour to population ecology* (Oxford University Press, Oxford ; New York, 1996).

25. Huh, W. K. et al. Global analysis of protein localization in budding yeast. *Nature* 425, 686-91 (2003).
26. Paulsson, J. Summing up the noise in gene networks. *Nature* 427, 415-8 (2004).
27. Gillespie, DT. Exact stochastic simulation of coupled chemical reactions. *J Phys Chem* 81, 2350 (1977).

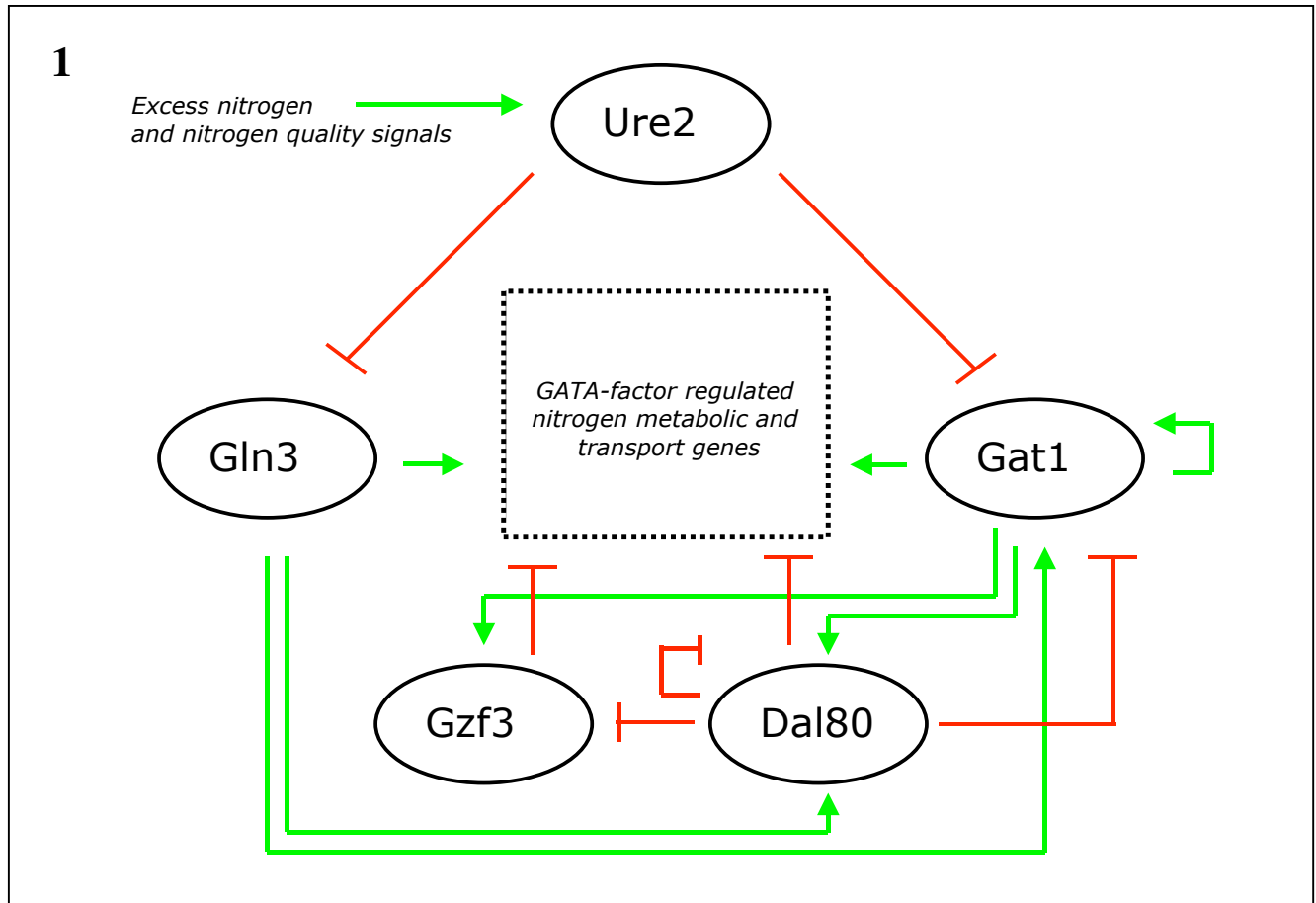


**Figure 1. Schematic of nitrogen regulation circuit in yeast.** Diagram of known interactions between four transcriptional regulators of nitrogen metabolism: Gln3p, Gat1p, Dal80p, and Gzf3p. Upstream kinases and other signals (from both the environment and inside the cell) of excess nitrogen and high nitrogen quality repress Gln3p and Gat1p by sequestering the transcription factors outside the nucleus with the Ure2p protein. In response to changes in nitrogen availability or quality, Gln3p and Gat1p induce the expression of Gzf3p and Dal80p, which in turn cross-regulate and auto-regulate the other factors as shown. These four regulators in turn regulate the set of nitrogen utilization genes (approximately 500). Due to complex and combinatorial interactions in the circuit as illustrated, as well as at the individual promoters of nitrogen utilization genes, expression can be up-regulated or down-regulated depending on the environment, and can be adjusted to meet environmental demands.

2a

Parent strain



Engineered strain



2b

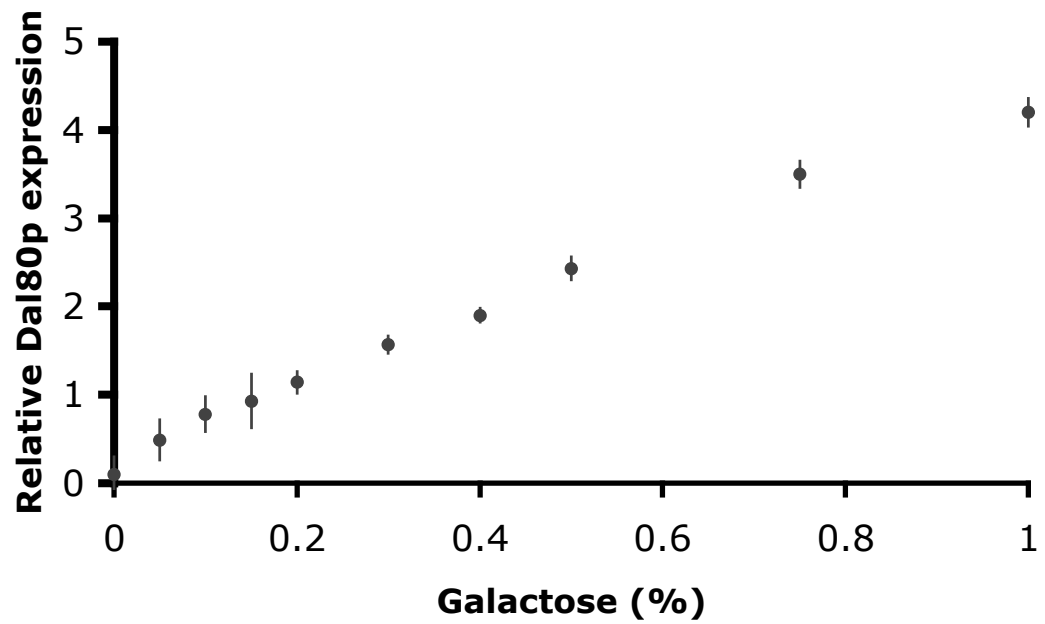
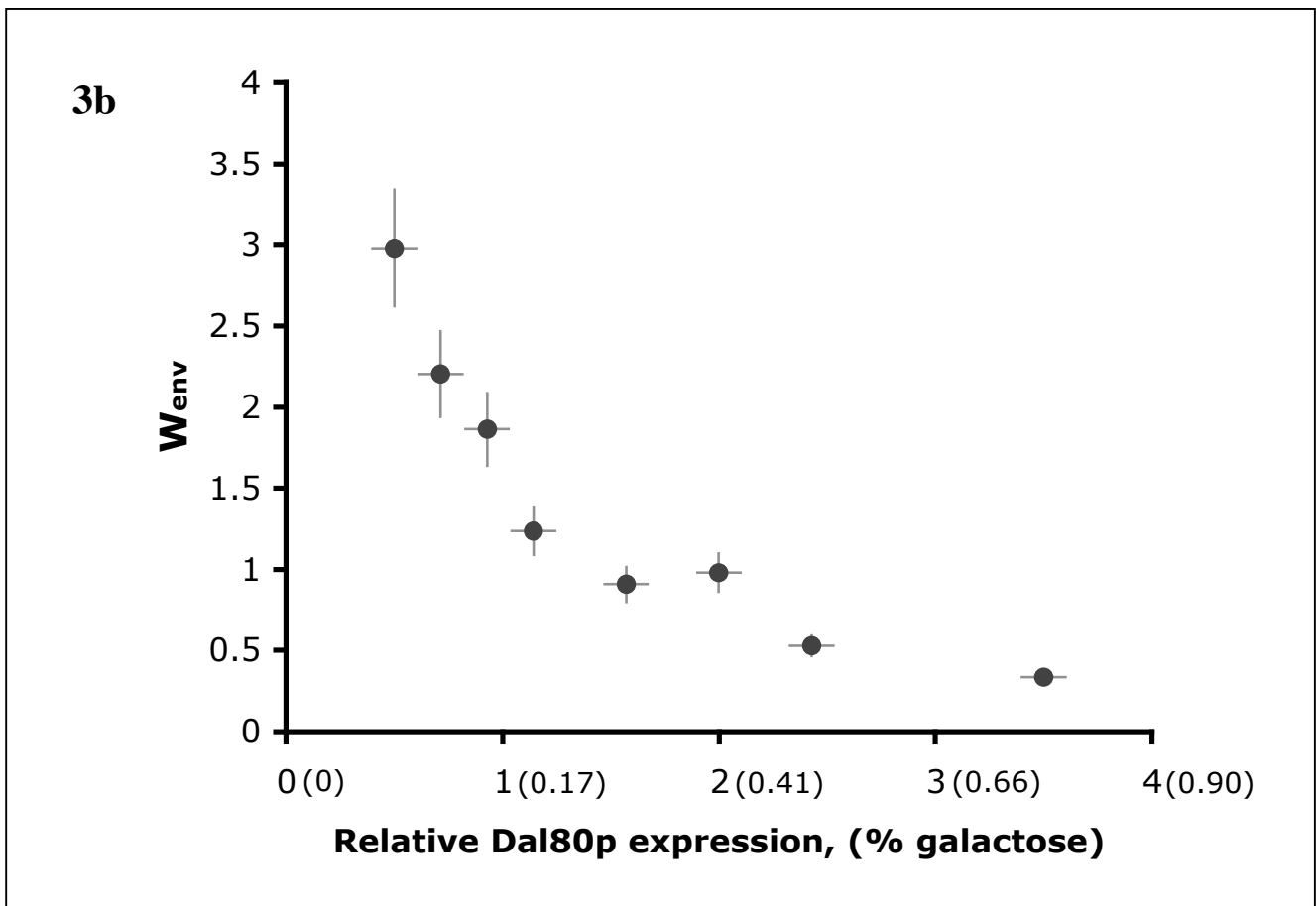
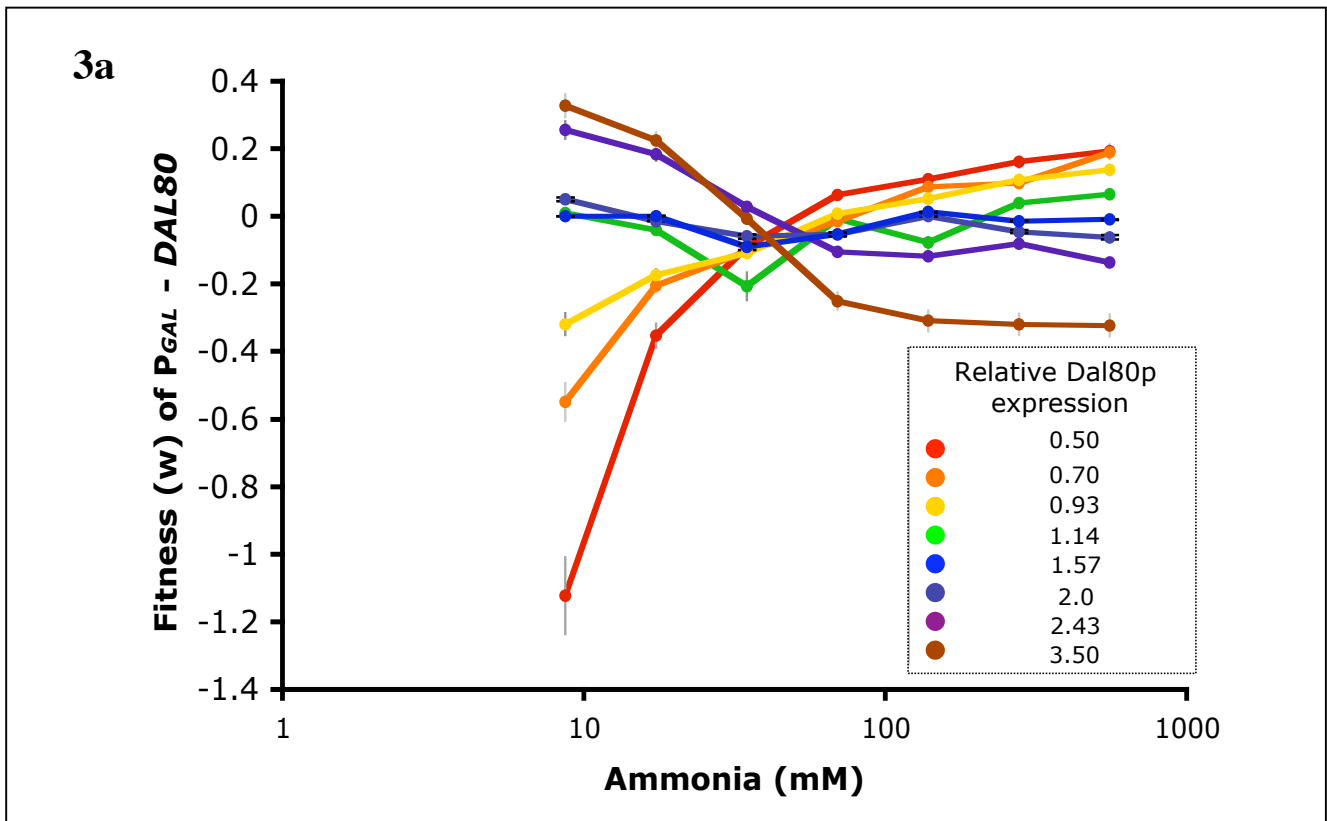


**Figure 2 Expression level of a transcriptional regulator determines competitive ability in varying ammonia concentrations.** **a**, The parent strain and engineered  $P_{GAL}$ -*DAL80* strain, where the endogenous *DAL80* promoter is replaced with the *GAL1-10* promoter. **b**, Tunable Dal80p expression as a function of galactose concentration for the engineered  $P_{GAL}$ -*DAL80* strain. Cells were grown overnight in non-inducing/non-repressing media (synthetic complete with 2% (wt/vol) sucrose, 1% raffinose), diluted 50-fold in the specified galactose concentration, and grown for 6 hours. Cells were harvested and total RNA was extracted as specified. Relative transcript levels were measured by reverse transcription and quantitative PCR (qRT-PCR). Relative *DAL80* transcript levels were normalized to relative *ACT1* transcript levels for each sample and are reported relative to the parent strain. The mean  $\pm$ s.d. from at least three independent experiments is shown.



**3a**, Fitness of the engineered strain across varying ammonia concentrations at different Dal80p expression levels. Dal80p expression was varied by altering the concentration of galactose in the media and measured by qRT-PCR, and is reported relative to parent Dal80p levels for each set of fitness data. Equal amounts of the reference and  $P_{GAL-DAL80}$  or parent strains were mixed and grown in the indicated ammonia and galactose concentrations. Numbers of each strain were quantitated through flow cytometry and fitness of the  $P_{GAL-DAL80}$  strain is reported as the natural log of the change in frequency over the growth period relative to the parent strain. **b**, Environment-dependent fitness parameter,  $W_{env}$ , of the  $P_{GAL-DAL80}$  strain as a function of Dal80p expression.  $W_{env}$  is calculated as the ratio of fitness in high ammonia (556 mM) to fitness in low ammonia (8.6 mM) relative to the parent strain.

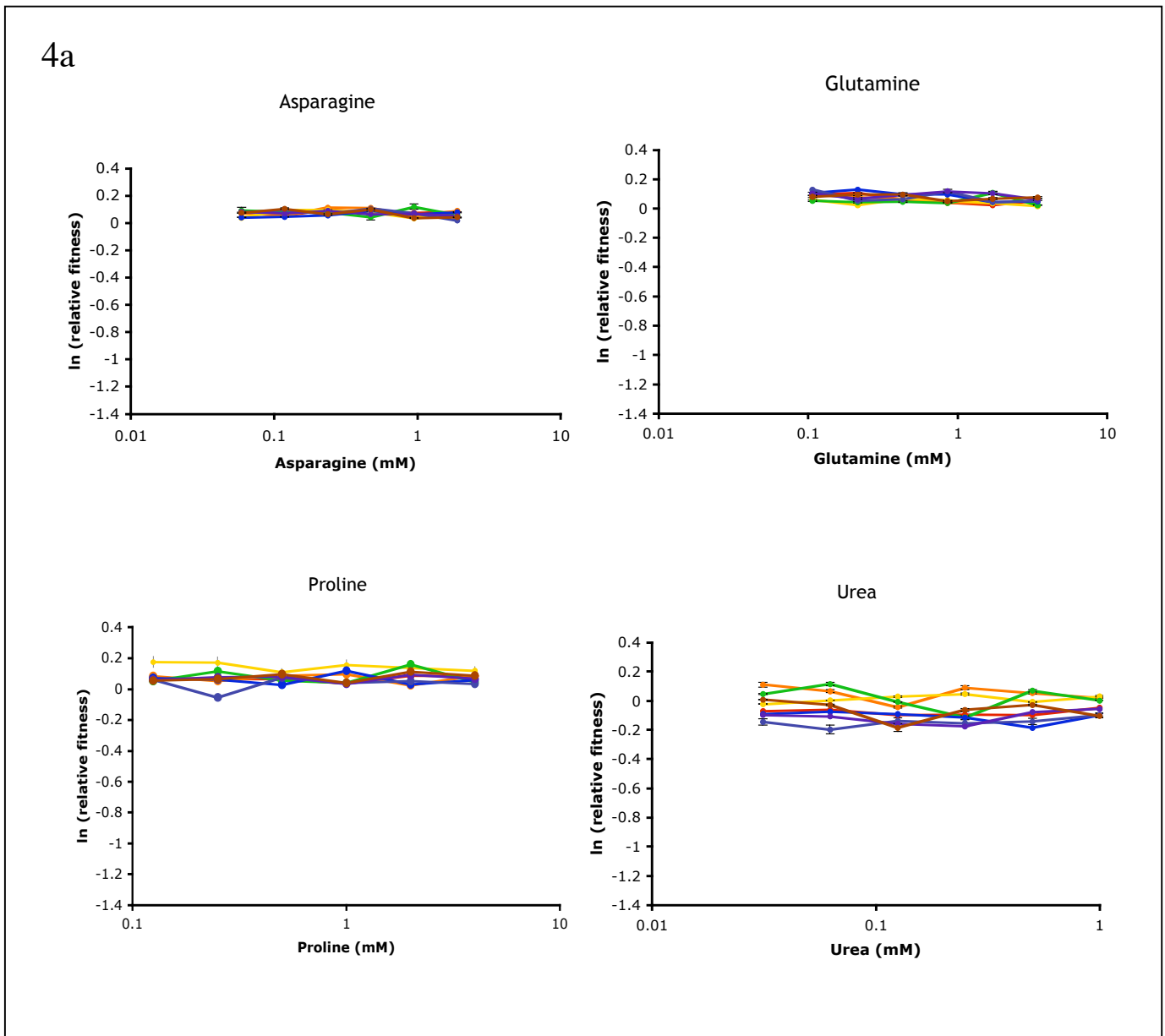


**Figure 4a** Fitness trends are specific to ammonia as the nitrogen source. Relative fitness of the engineered  $P_{GAL}\text{-DAL80}$  strain in alternative nitrogen sources at different Dal80p expression levels. Fitness trends are reported across varying concentrations of preferred nitrogen sources (asparagine and glutamine) and non-preferred nitrogen sources (proline and urea). Colors represent relative Dal80p expression levels as indicated in Figure 1b. Competitive fitness shows little change relative to the parent strain in either preferred or non-preferred nitrogen sources. The mean  $\pm$ s.d. from at least three independent experiments is shown for all data.

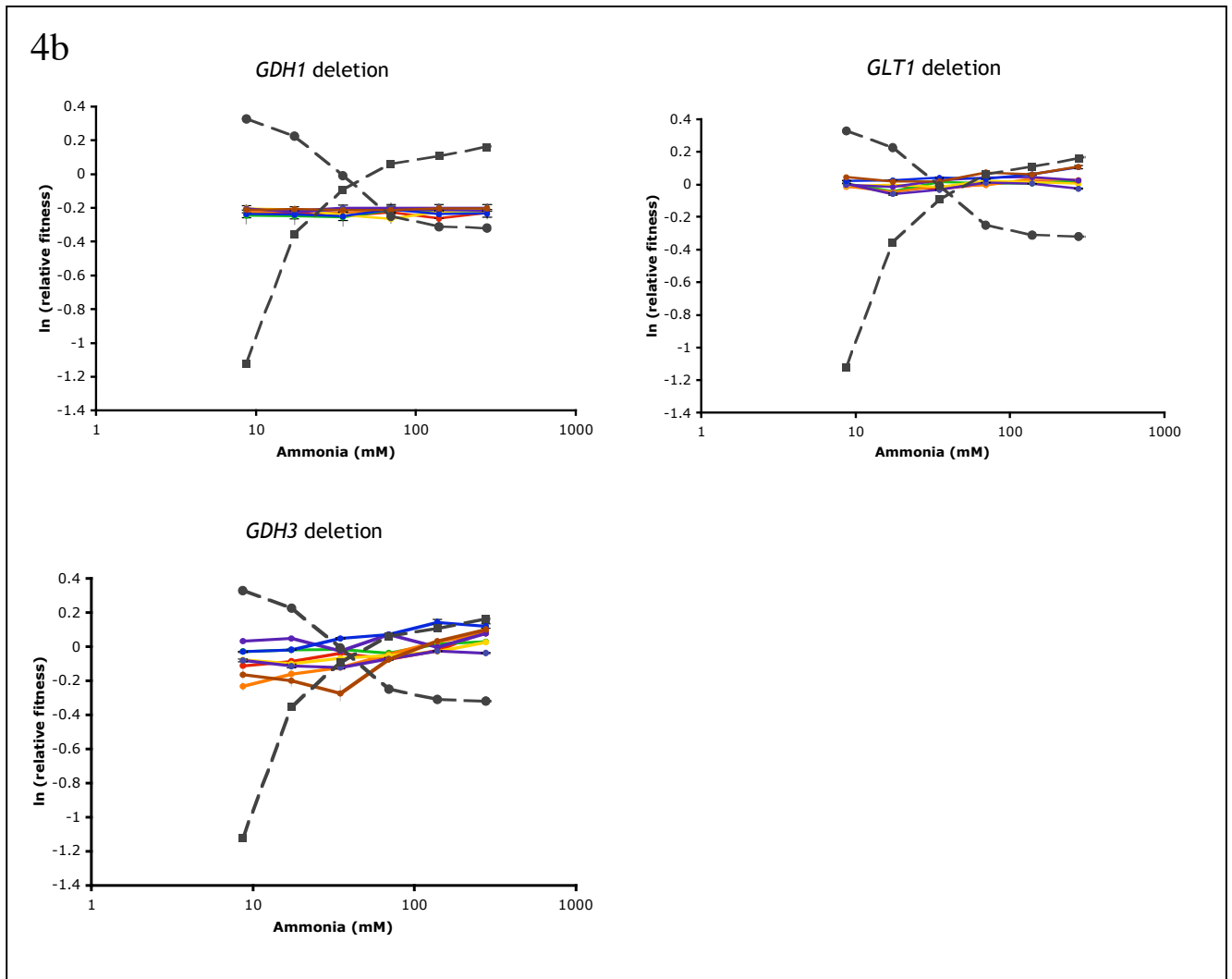
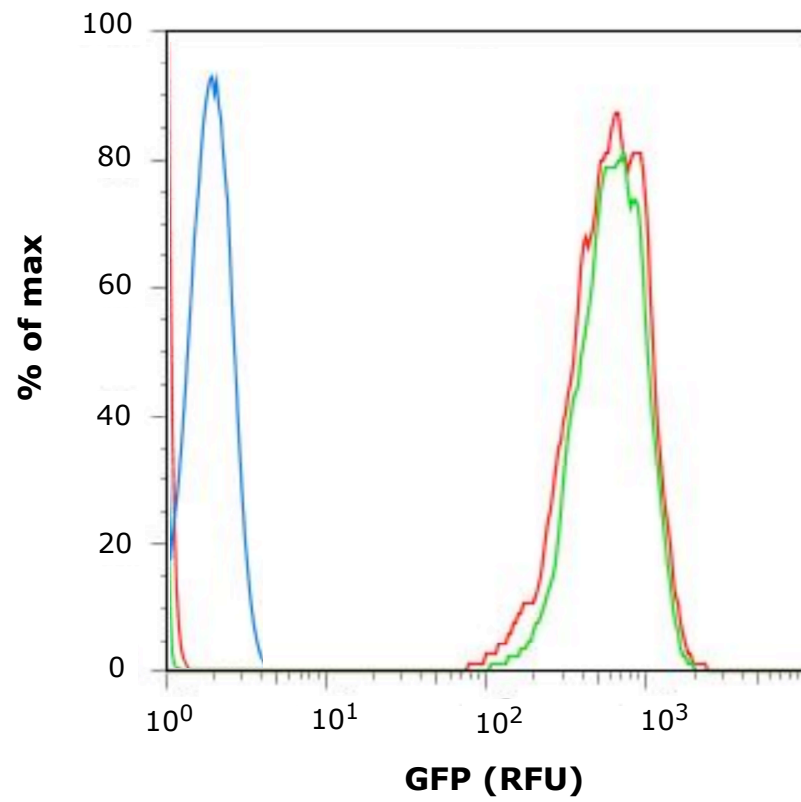
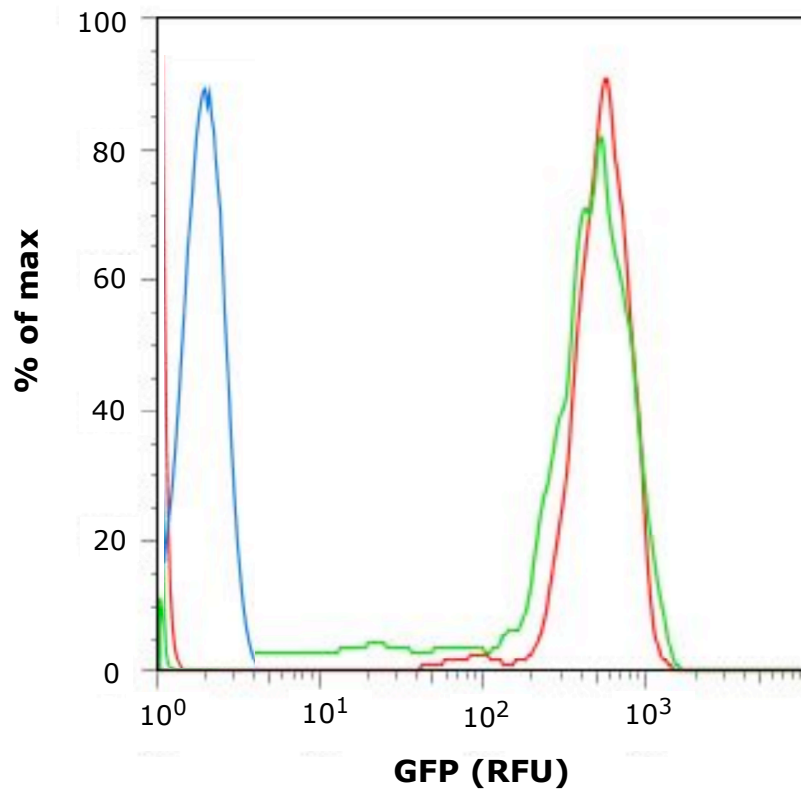


**Figure 4b Fitness trends require all three ammonia assimilation pathways.** Fitness trends for the  $P_{GAL}\text{-DAL80 } gdh1\Delta$ ,  $P_{GAL}\text{-DAL80 } glt1\Delta$ , and  $P_{GAL}\text{-DAL80 } gdh3\Delta$  strains across varying ammonia concentrations at different Dal80p expression levels. Dashed lines represent relative fitness of the engineered strain ( $P_{GAL}\text{-DAL80}$ ) across varying ammonia concentrations for low Dal80p (squares, 0.5-fold parent strain) and high Dal80p (circles, 3.5-fold parent strain) expression levels for comparison. The observed fitness trends are abolished in the  $P_{GAL}\text{-DAL80 } gdh1\Delta$  strain, and fitness across all ammonia concentrations is lower than the parent strain. Fitness trends are absent in the  $P_{GAL}\text{-DAL80 } glt1\Delta$  strain similar to the Gdh1p deletion. Fitness values slightly increase with ammonia concentration in the  $P_{GAL}\text{-DAL80 } gdh3\Delta$  strain, although fitness trends are similarly abolished. The mean  $\pm$ s.d. from at least three independent experiments is shown for all data.

5a



5b



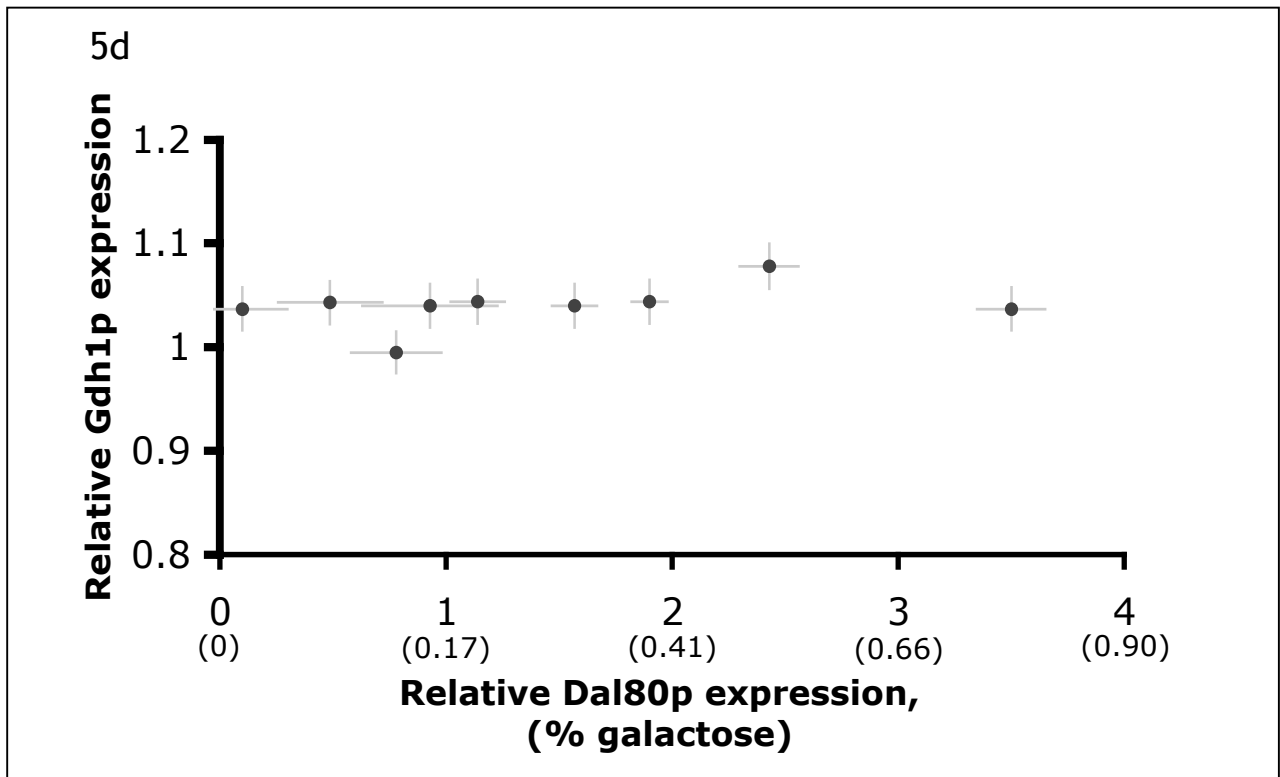
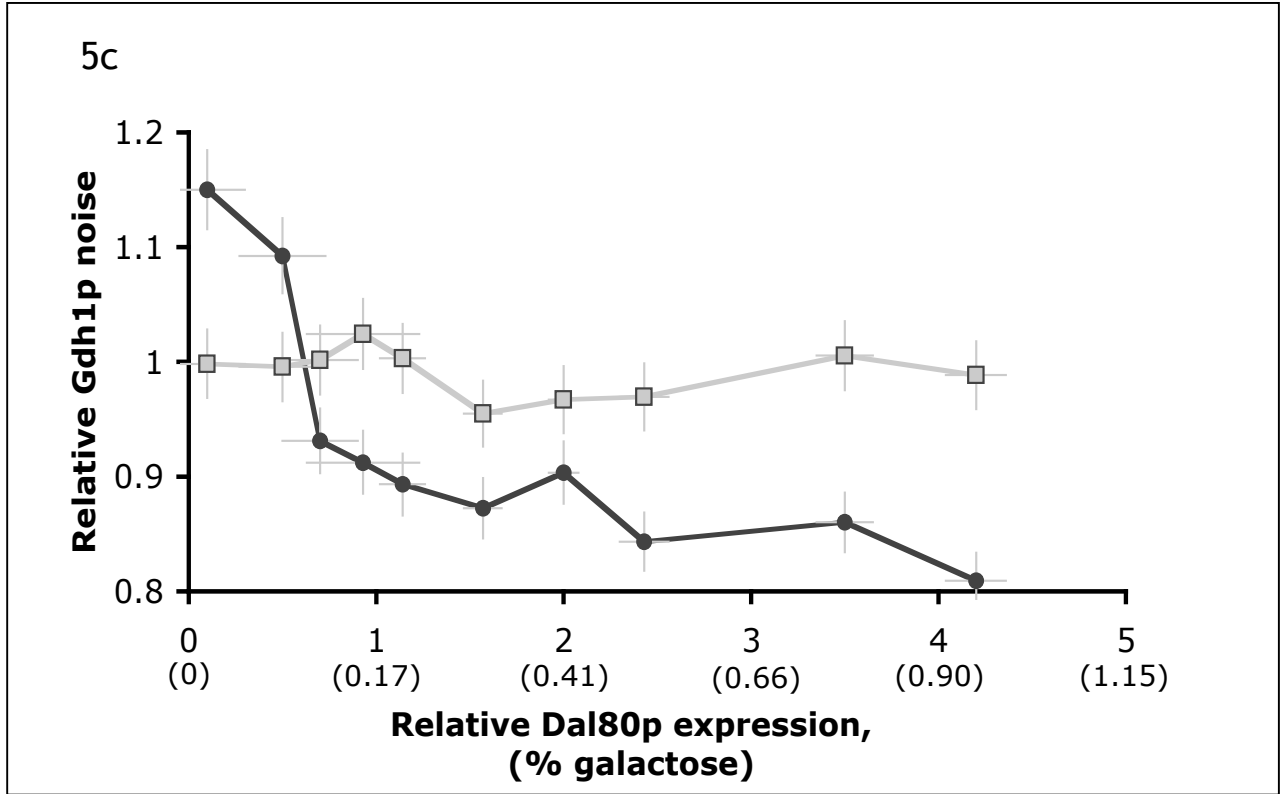


**Figure 5a**, Representative histogram of Gdh1p expression at 0% in wildtype (green),  $P_{GAL}$ -*DAL80* cells at 0% galactose (red), and cellular autofluorescence (W303 $\alpha$ , blue). **b**, Representative histogram of Gdh1p expression at 0% in wildtype (green),  $P_{GAL}$ -*DAL80* cells at 0% galactose (red), and cellular autofluorescence (W303 $\alpha$ , blue). **c**, Noise in Gdh1p:GFP expression in the  $P_{GAL}$ -*DAL80* strain (black) and parent strain (grey) with varying Dal80p levels. Noise values are reported relative to the parent strain at 0% galactose. **d**, Gdh1p expression levels in the  $P_{GAL}$ -*DAL80* strain with varying Dal80p levels. The arithmetic mean of the fluorescence population distribution relative to the parent strain is shown, and displays little change as Dal80p levels are increased.

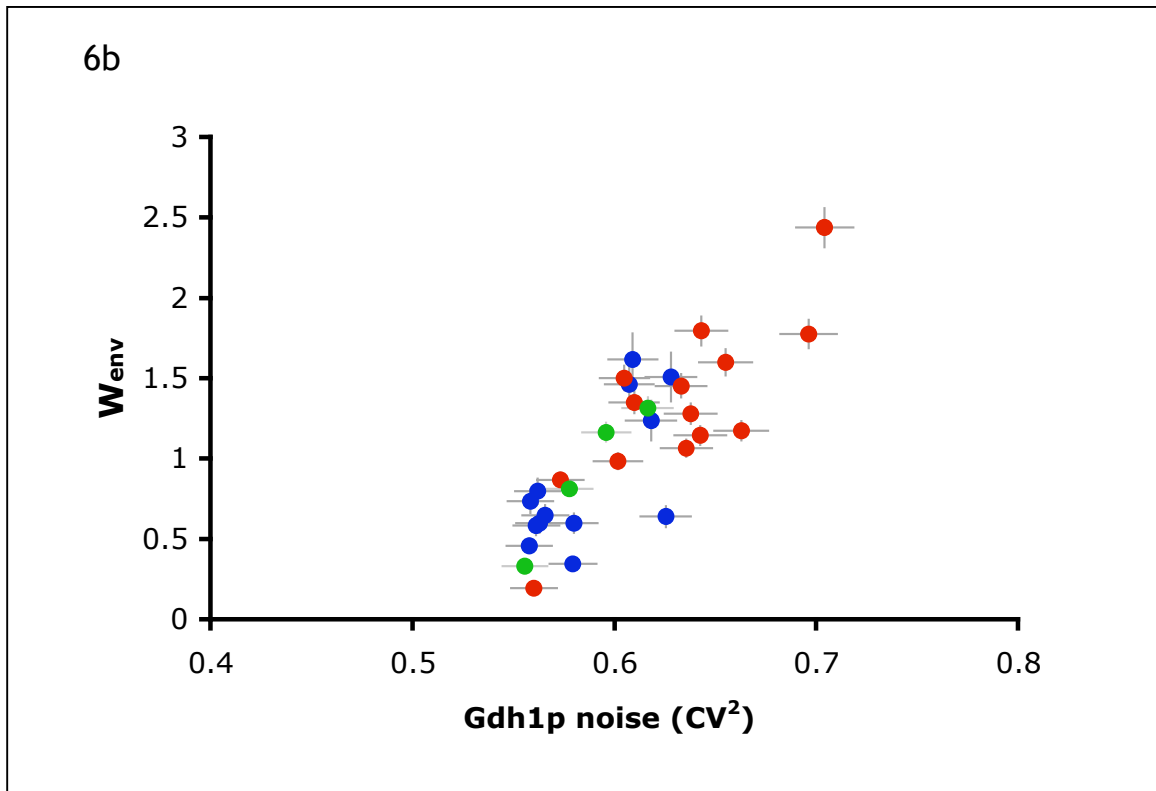
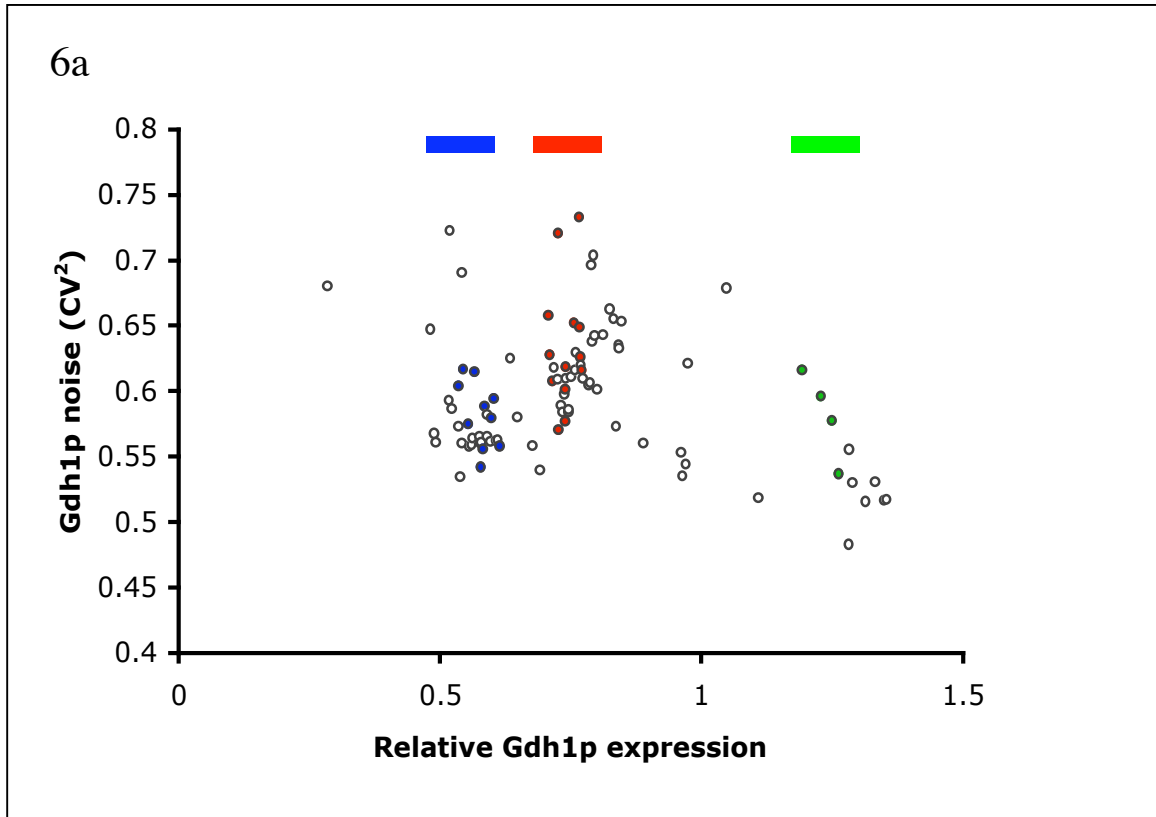


**Figure 6** *GDH1* promoter mutants show a range of Gdh1p abundance versus noise values. **a**, Noise in Gdh1p expression versus mean Gdh1p abundance for a set of randomly selected *GDH1* promoter mutants ( $n = 91$ ). Red, blue, and green bars indicate mutant sets having similar Gdh1p abundances (low, medium, and high, respectively) over a range of noise values. All errors are within 5% of the reported values. **b**,  $W_{\text{env}}$  versus noise in Gdh1p expression for the highlighted mutant sets. Mutant sets with low (red), medium (blue), and high (green) Gdh1p abundance levels are indicated.

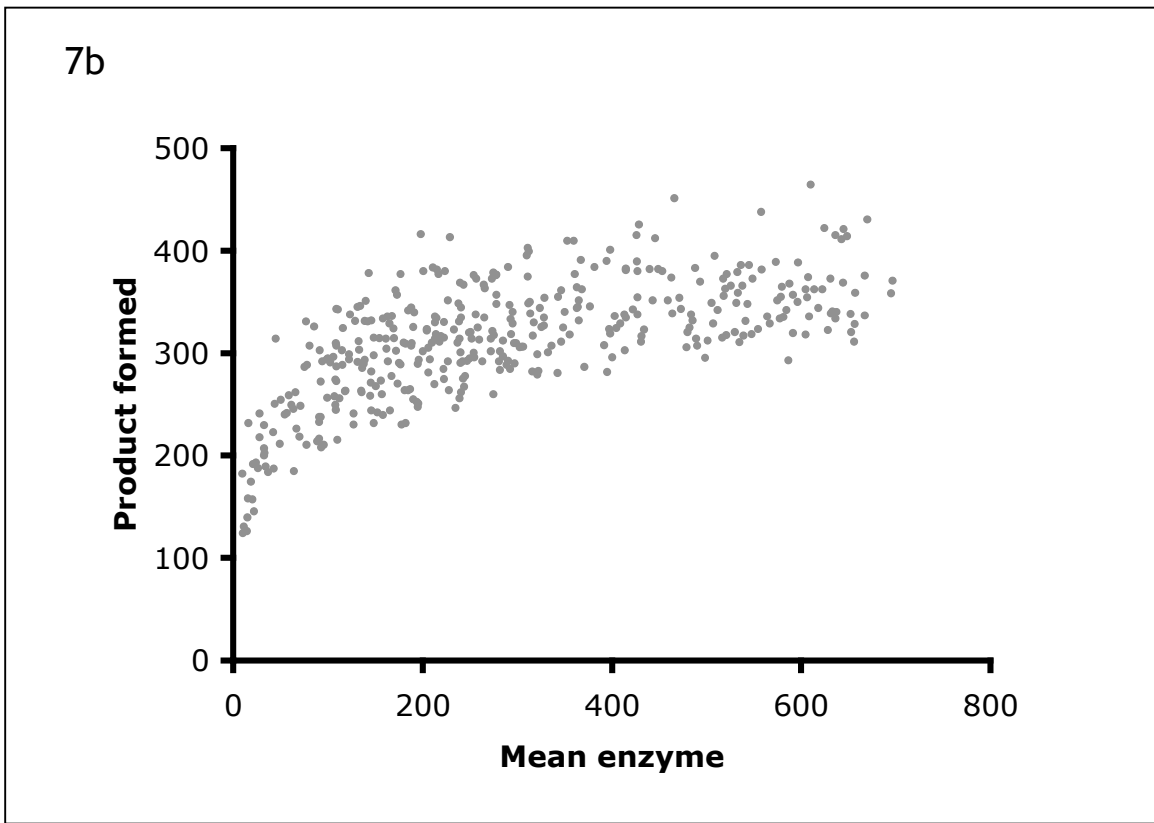
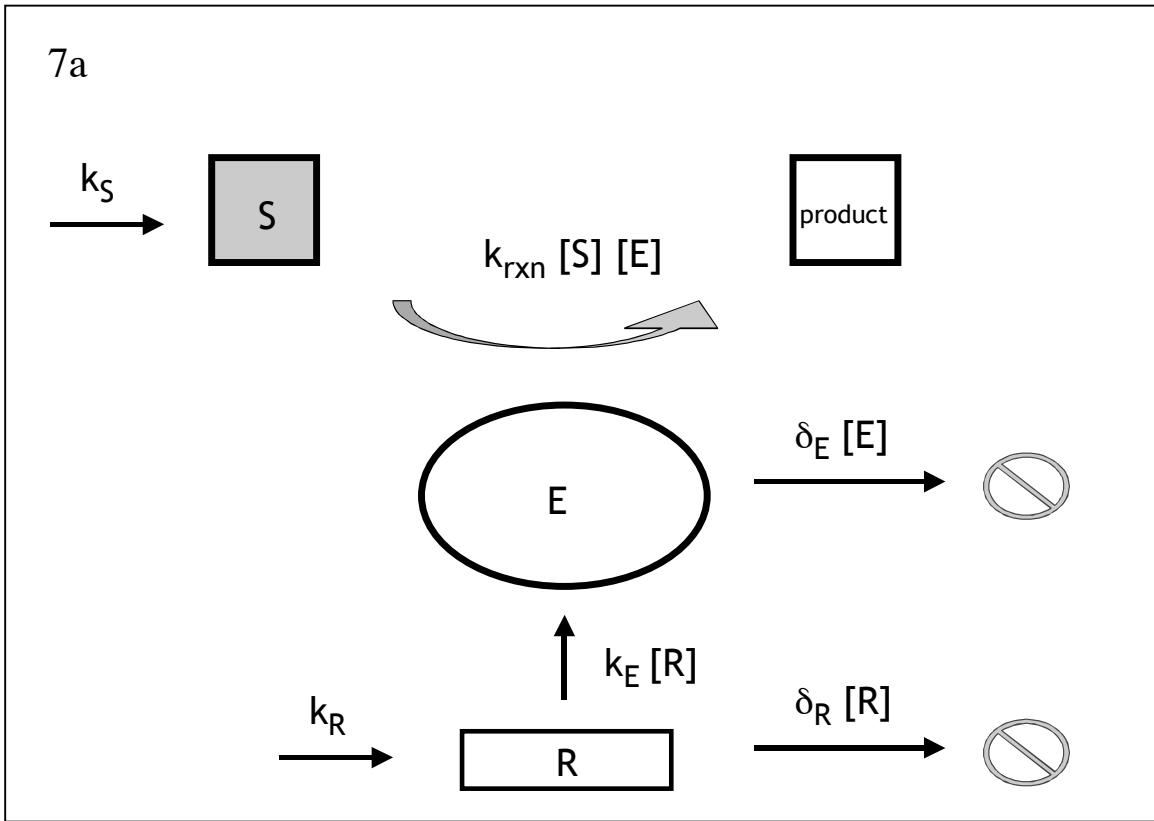


**Figure 7 Schematic of enzyme reaction simulation.** **a**, schematic for the simulated enzyme reactions is shown. In the specified system, mRNA is produced at a constant rate and decays at a rate proportional to its concentration. Enzyme is produced at a rate proportional to the mRNA concentration and decays at a rate proportional to its concentration. Substrate is imported at a constant rate and is converted to product at a rate dependent on the substrate and enzyme concentrations. The rate of product formation in this system can be determined from the amount of product formed over the run time of the simulation. **b**, Simulation results showing product formation as a function of enzyme abundance with other parameters held constant. Product formation shows canonical hyperbolic dependence on enzyme levels with a plateau region at mean enzyme levels greater than 80.

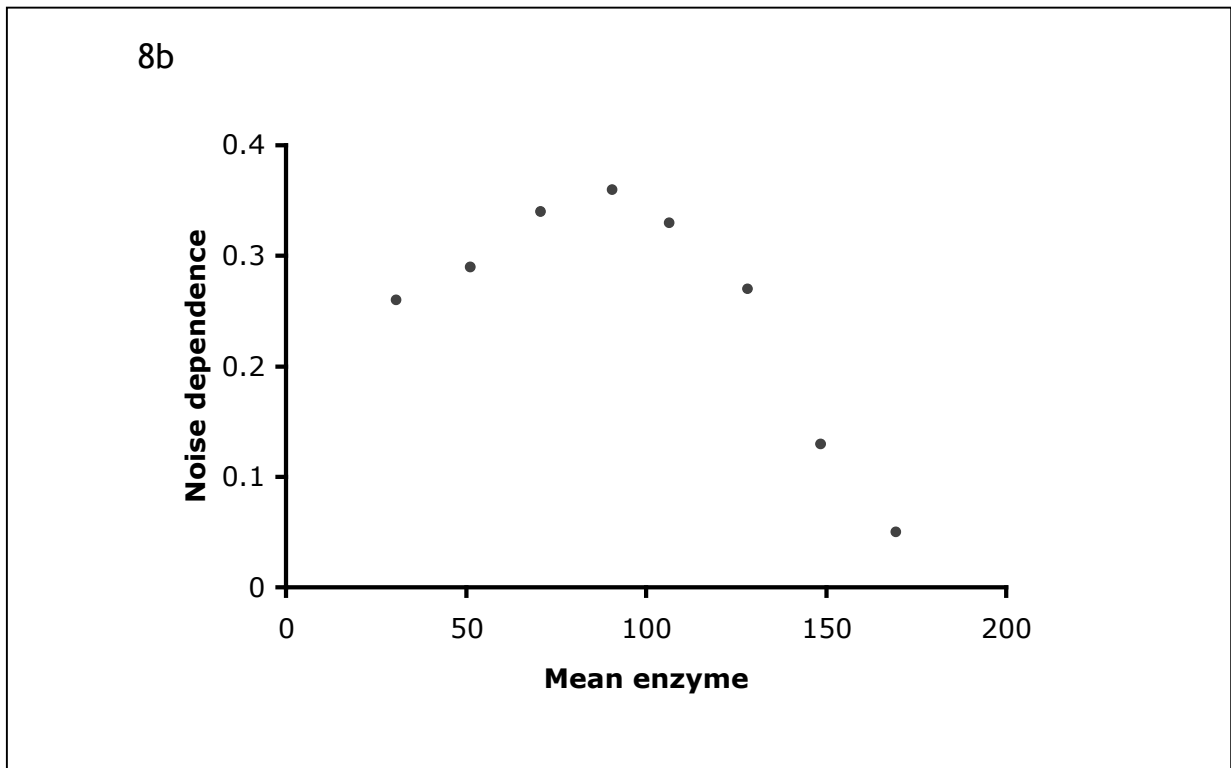
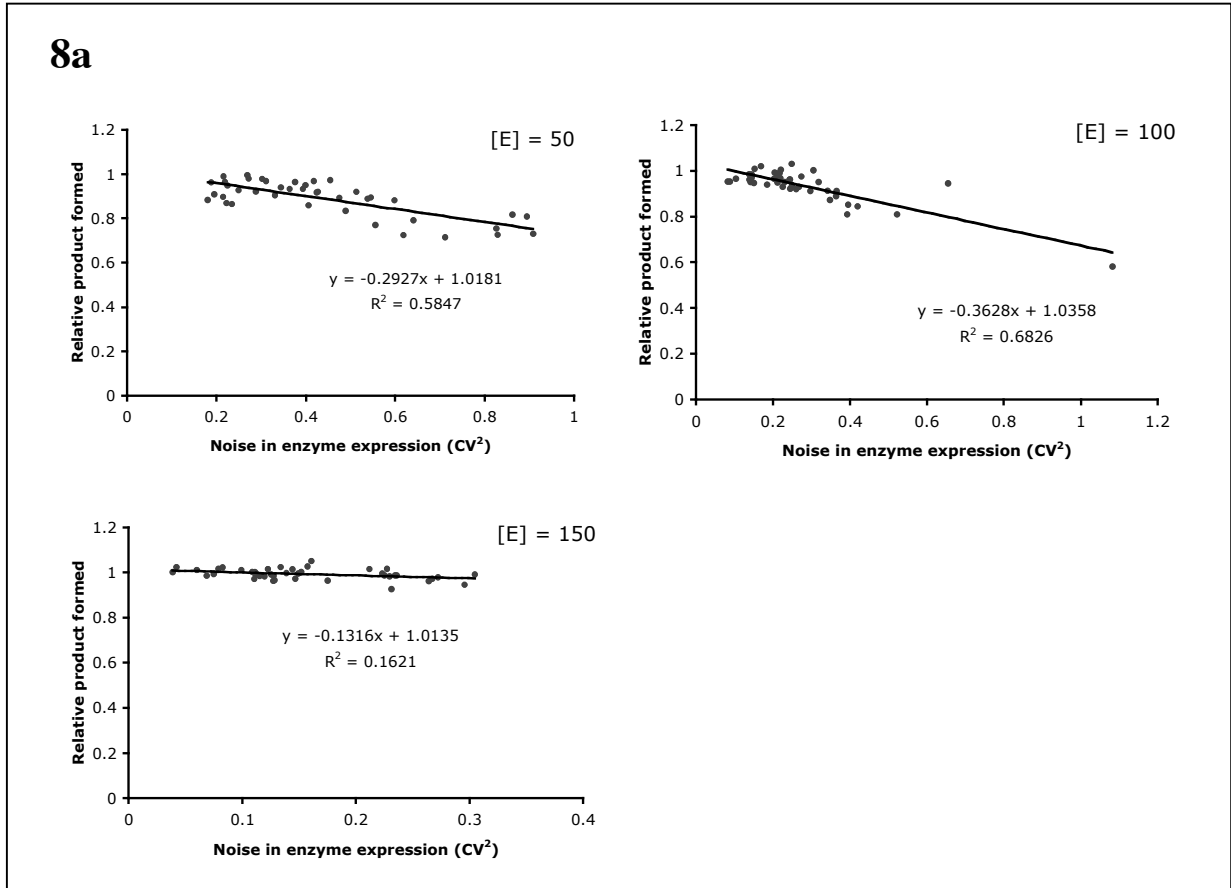


**Figure 8 The dependence of product formation on the noise in enzyme expression in a simulated enzyme reaction system.** **a**, the dependence of product formation on noise in enzyme expression at different enzyme abundances for the simulated system is shown. Noise was varied by changing the ratio of  $\delta R$  (mRNA decay rate) to  $kE$  (enzyme translation rate), which varies the average number of proteins translated from a single mRNA (burst size), and mRNA synthesis rates were adjusted accordingly to have similar enzyme abundances between simulations. The slope of the product formation versus noise trend represents the noise susceptibility at this enzyme concentration. Simulations are shown for three mean enzyme abundances ( $[E] = 50, 100, \text{ and } 150$ ). **b**, Noise dependence of product formation as a function of enzyme expression for the simulated enzyme system. Noise was varied by changing the average number of proteins translated from a single mRNA (burst size), while compensating the rate of RNA production to retain similar mean abundances between simulations. The slope of the product formed versus noise trend for each abundance level represents the noise dependence at this enzyme abundance.

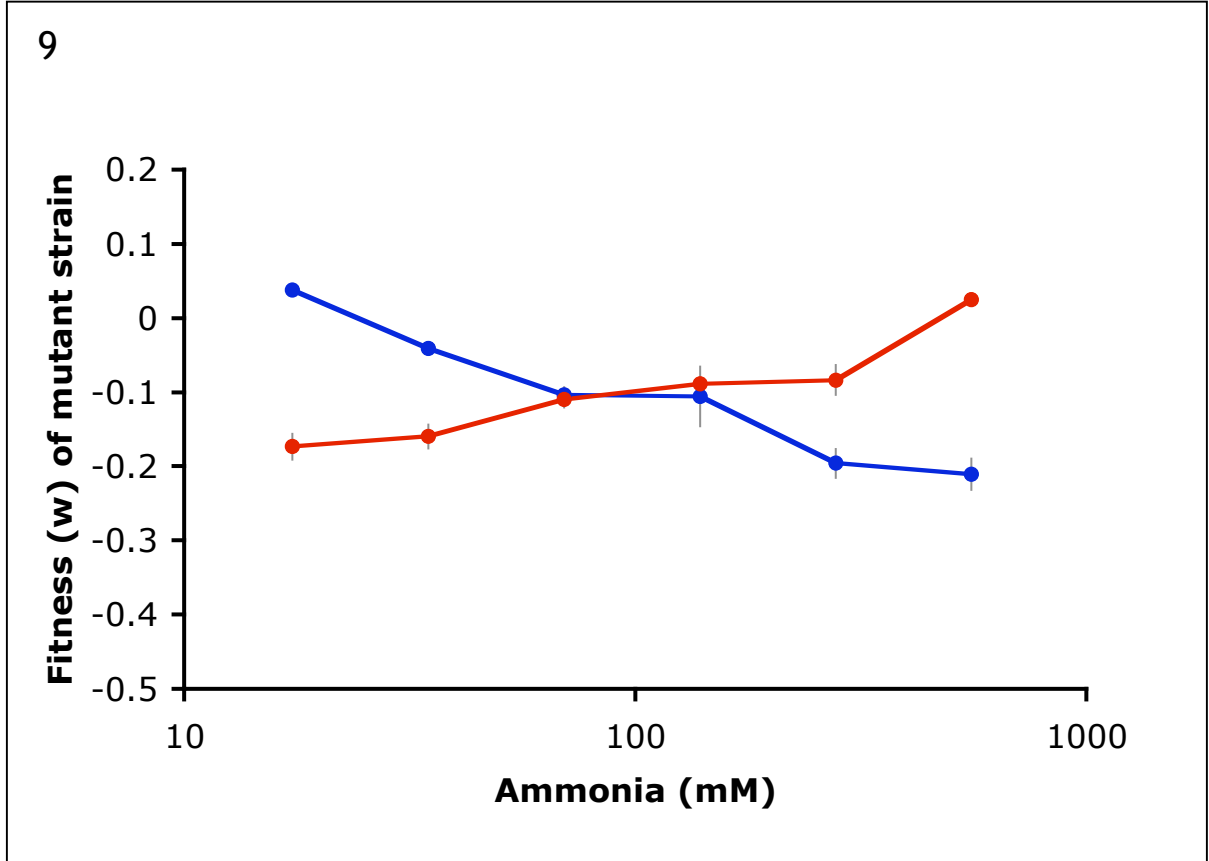


**Figure 9.** Fitness of the rate-deficient D150H (red) and rate-enhanced C313S (blue) strains relative to the parent strain across varying ammonia concentrations. Fitness was assayed as above.

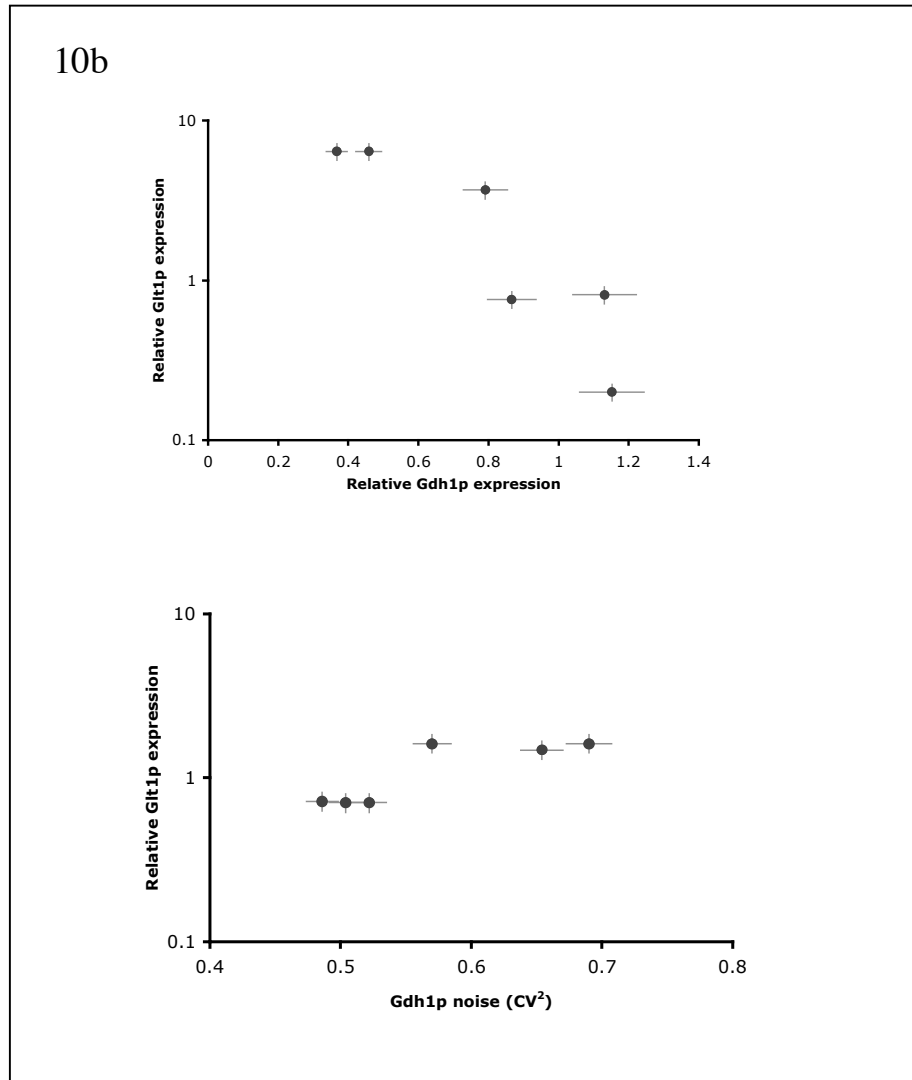
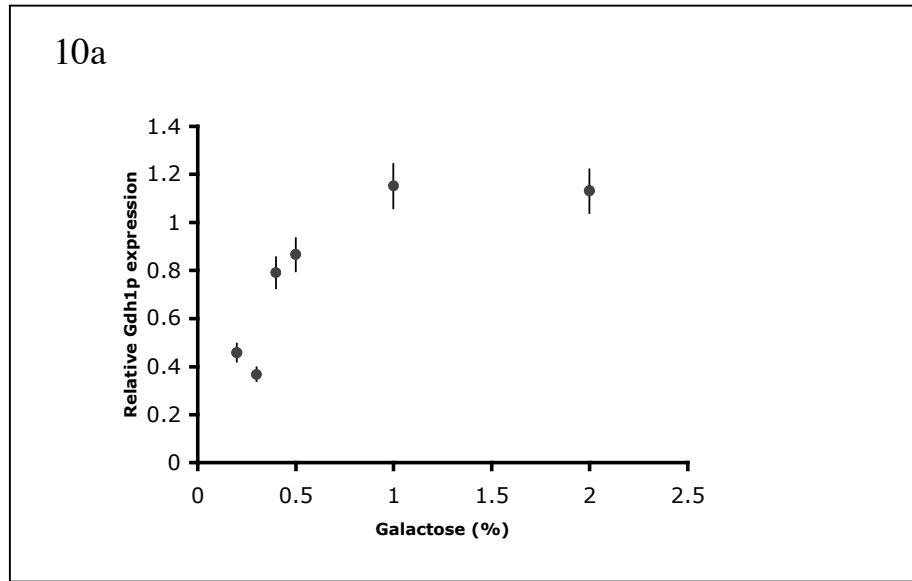


**Figure 10a Tunable Gdh1p expression as a function of galactose concentration for the engineered  $P_{GAL}$ -*GDH1* strain.** Relative Gdh1p:GFP levels were measured as before and are reported relative to the parent strain. The mean  $\pm$ s.d. from at least three independent experiments is shown. **b, Glt1p expression varies with Gdh1p abundance rather than noise. Top,** Abundance of *GLT1* mRNA as a function of Gdh1p abundance. The endogenous *GDH1* promoter was replaced with the *GALI-10* promoter to achieve galactose tunable expression of Gdh1p. Cells were grown in varying galactose concentrations and Gdh1p:GFP expression was measured by flow cytometry as above. Cells were then harvested and *GLT1* mRNA was measured by qRT-PCR. *GLT1* transcript levels show an inverse relationship with Gdh1p abundance, suggesting that cellular regulatory mechanisms act to balance the expression of Gdh1p and Glt1p. **Bottom,** Abundance of *GLT1* mRNA as a function of noise in Gdh1p expression. The engineered galactose tunable Dal80p strain ( $P_{GAL}$ -*DAL80*), was used to modulate noise in Gdh1p expression while keeping abundance levels relatively unchanged. *GLT1* transcript levels show little change with varying Gdh1p noise. The mean  $\pm$ s.d. from at least three independent experiments is shown.

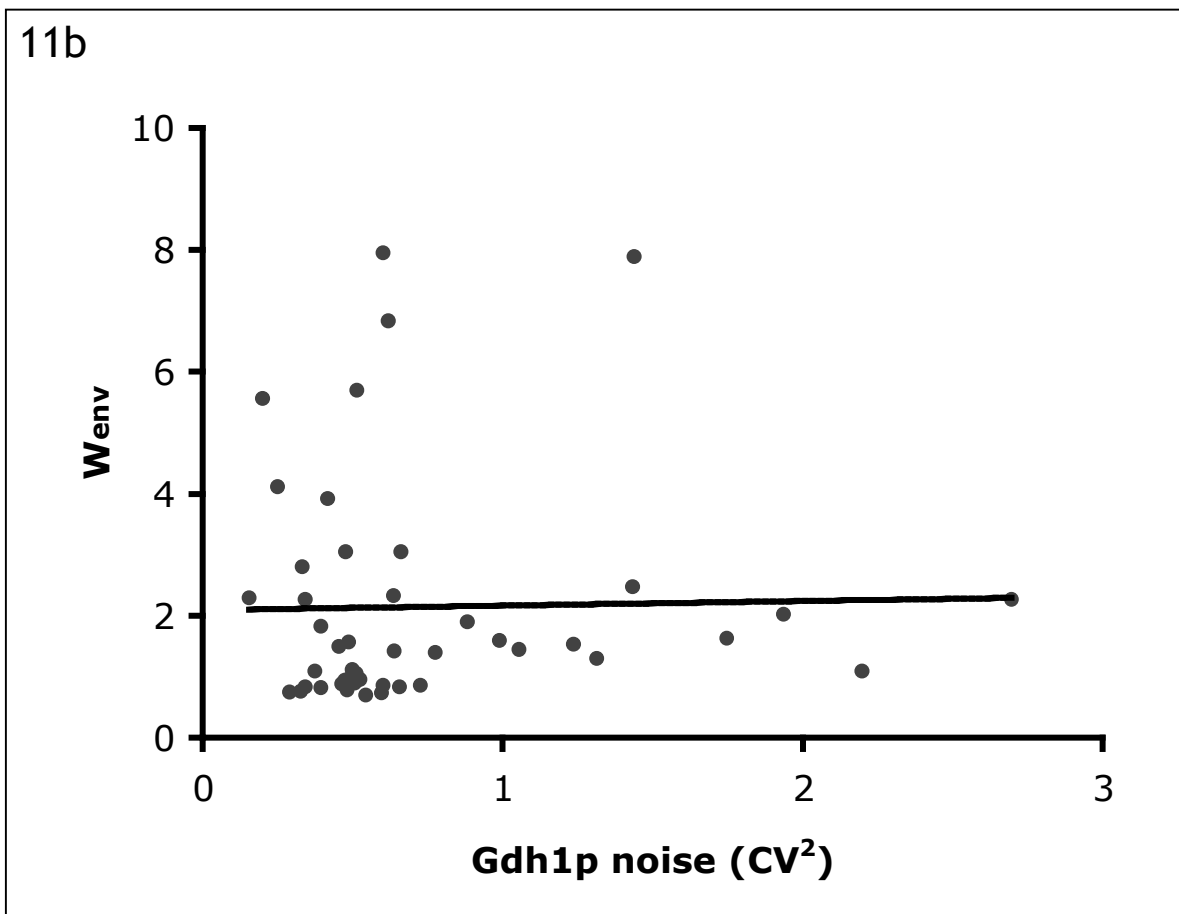
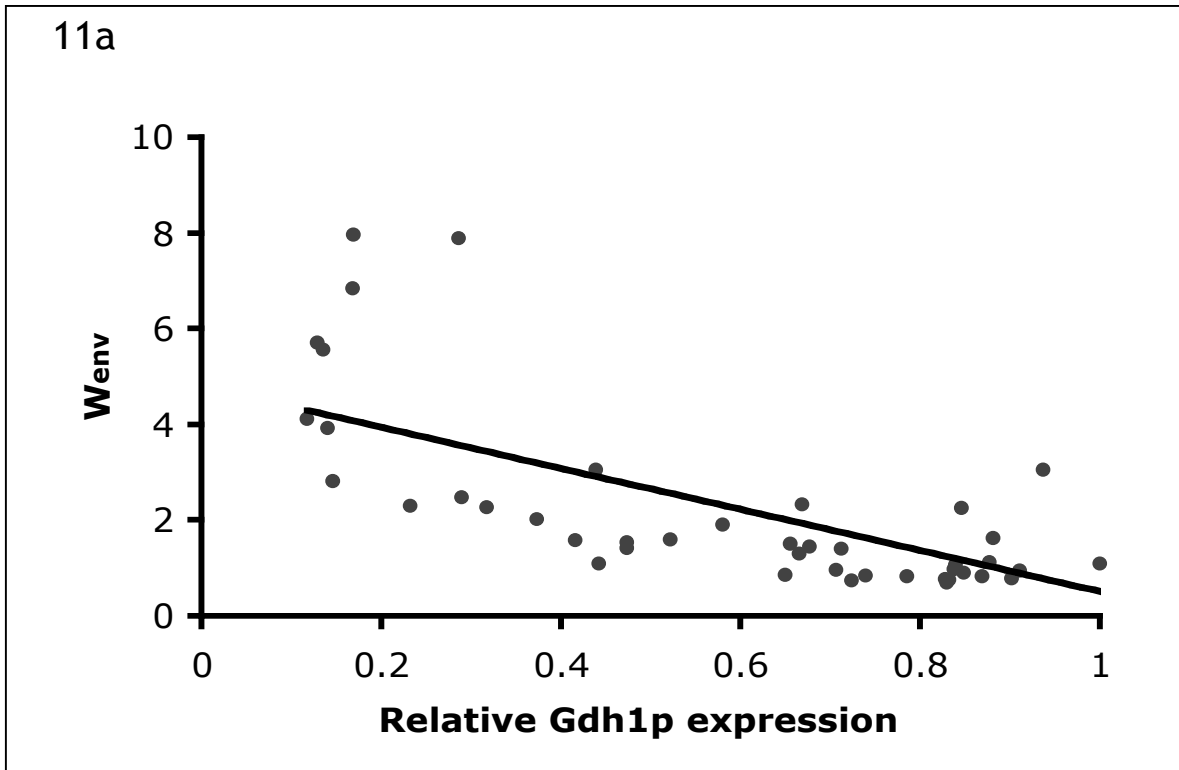


**Figure 11 The alternate assimilation enzyme Glt1p determines the effect of Gdh1p noise and abundance on fitness. a,** Abundance in  $W_{env}$  versus Gdh1p expression for a sampling of strains harboring the *GDH1* promoter library in a Gdh1p:GFP *GLT1Δ* background.  $W_{env}$  shows a negative correlation with abundance. **b,**  $W_{env}$  versus noise in Gdh1p expression for the same mutant set.  $W_{env}$  shows little correlation with noise in this mutant set.

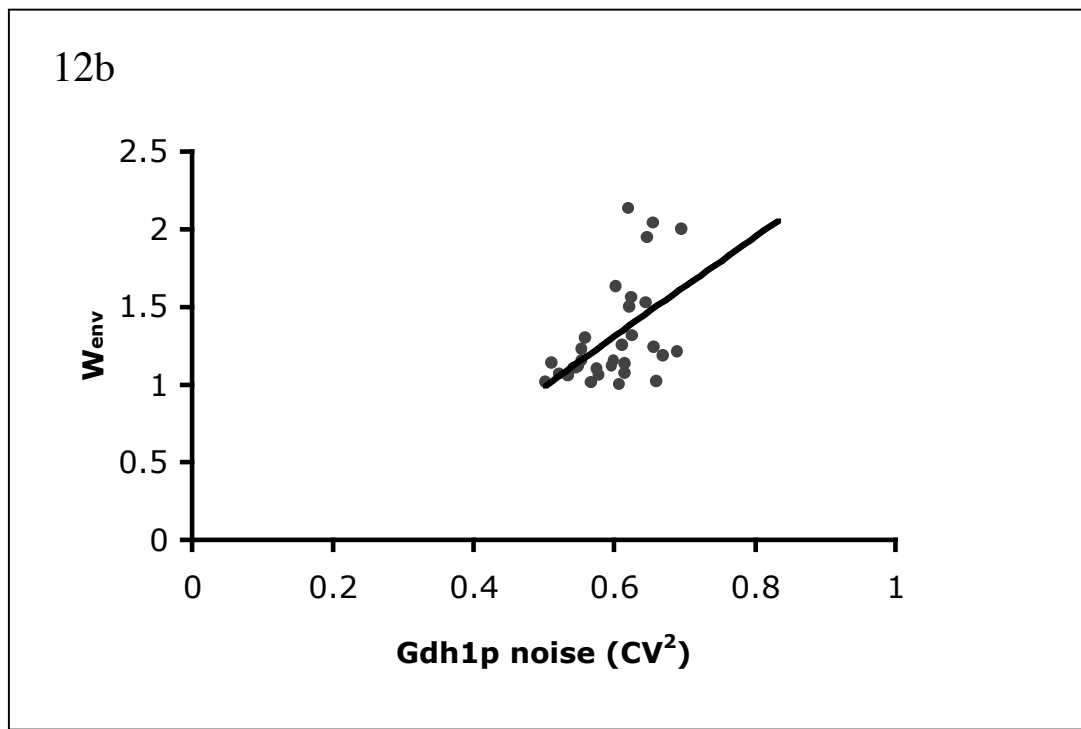
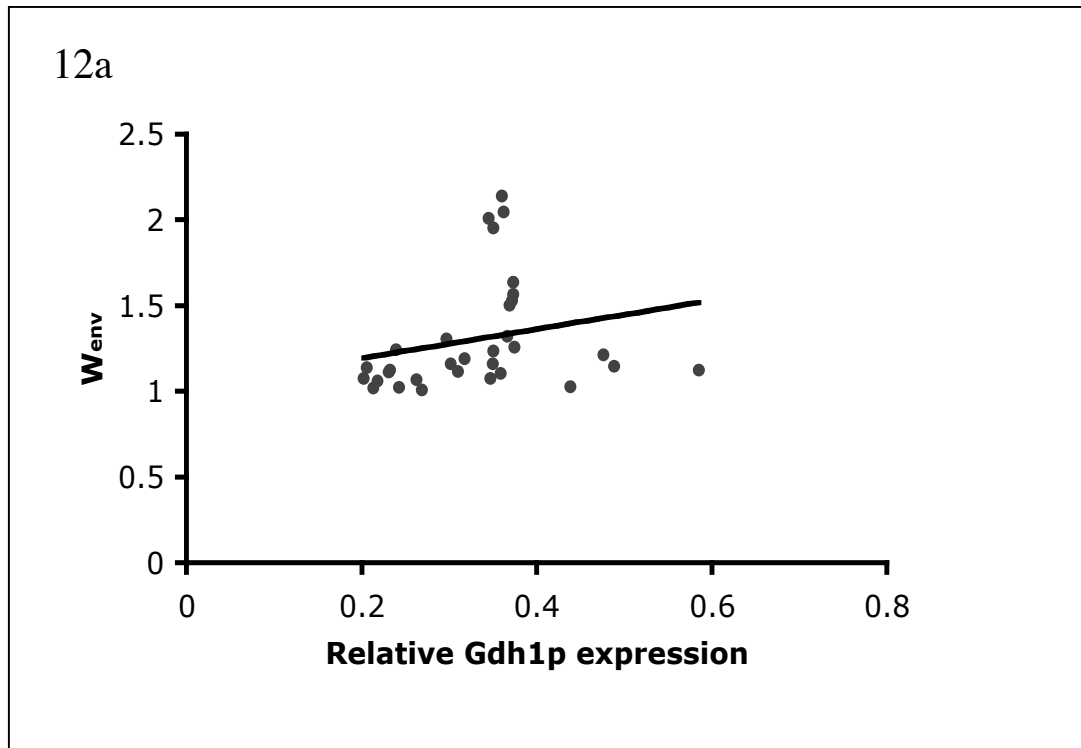


**Figure 12**  $W_{\text{env}}$  versus noise and abundance for *GDH1* promoter mutants in the wildtype background. **a**, Abundance in  $W_{\text{env}}$  versus Gdh1p expression for a sampling of strains harboring the *GDH1* promoter library in a Gdh1p:GFP background.  $W_{\text{env}}$  shows little correlation with abundance. The mean  $\pm$ s.d. from at least three independent experiments is shown. **b**,  $W_{\text{env}}$  versus noise in Gdh1p expression for the same mutant set.  $W_{\text{env}}$  shows stronger correlation with noise in this mutant set.

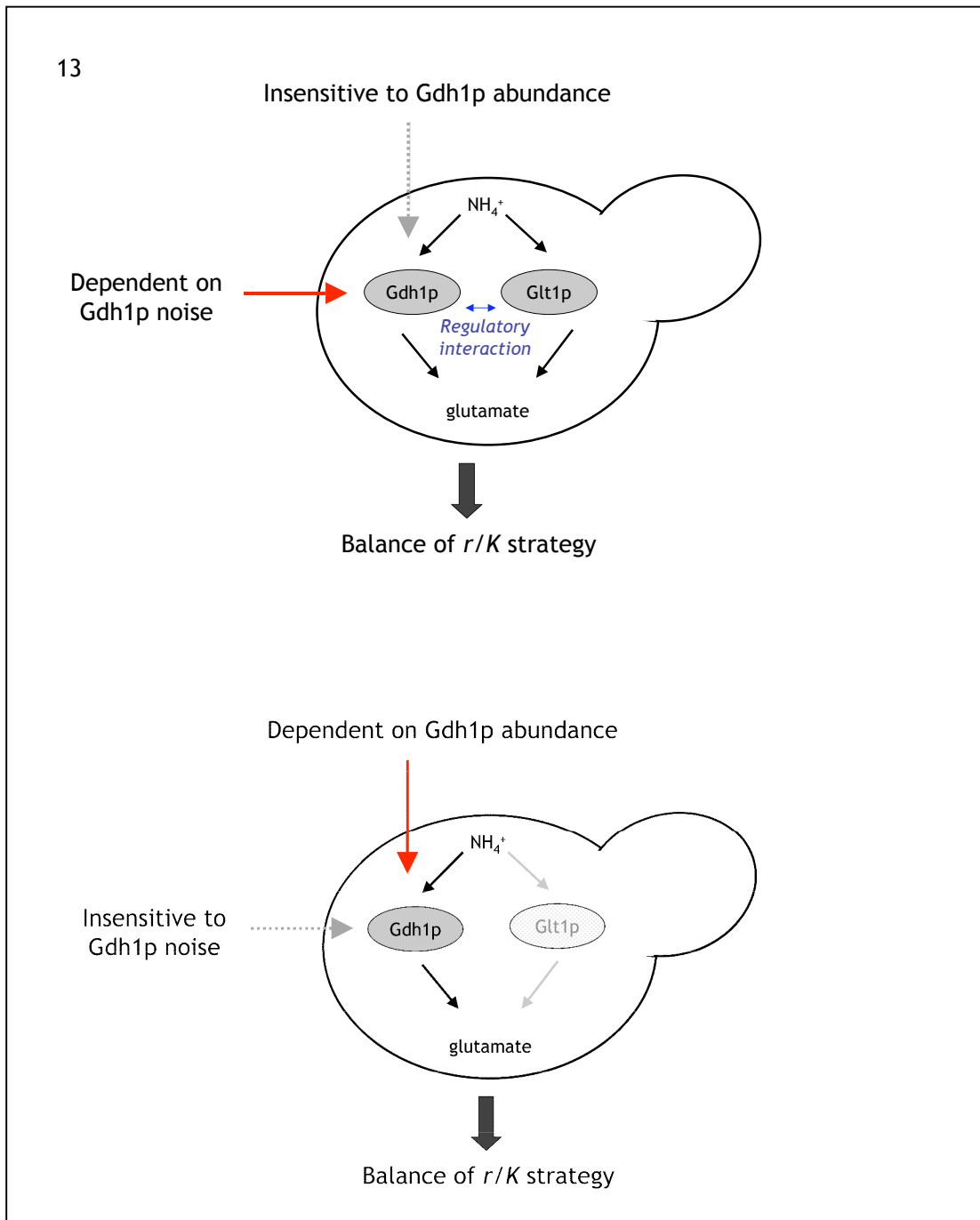


**Figure 13.** Representation of the effects of Gdh1p noise and abundance in the presence or absence of Glt1p. In the presence of both pathways noise in Gdh1p affects fitness because (uncharacterized) regulatory networks enable Glt1p to compensate for changes in Gdh1p abundance. In the absence of Glt1p the mean abundance of Gdh1p determines fitness.

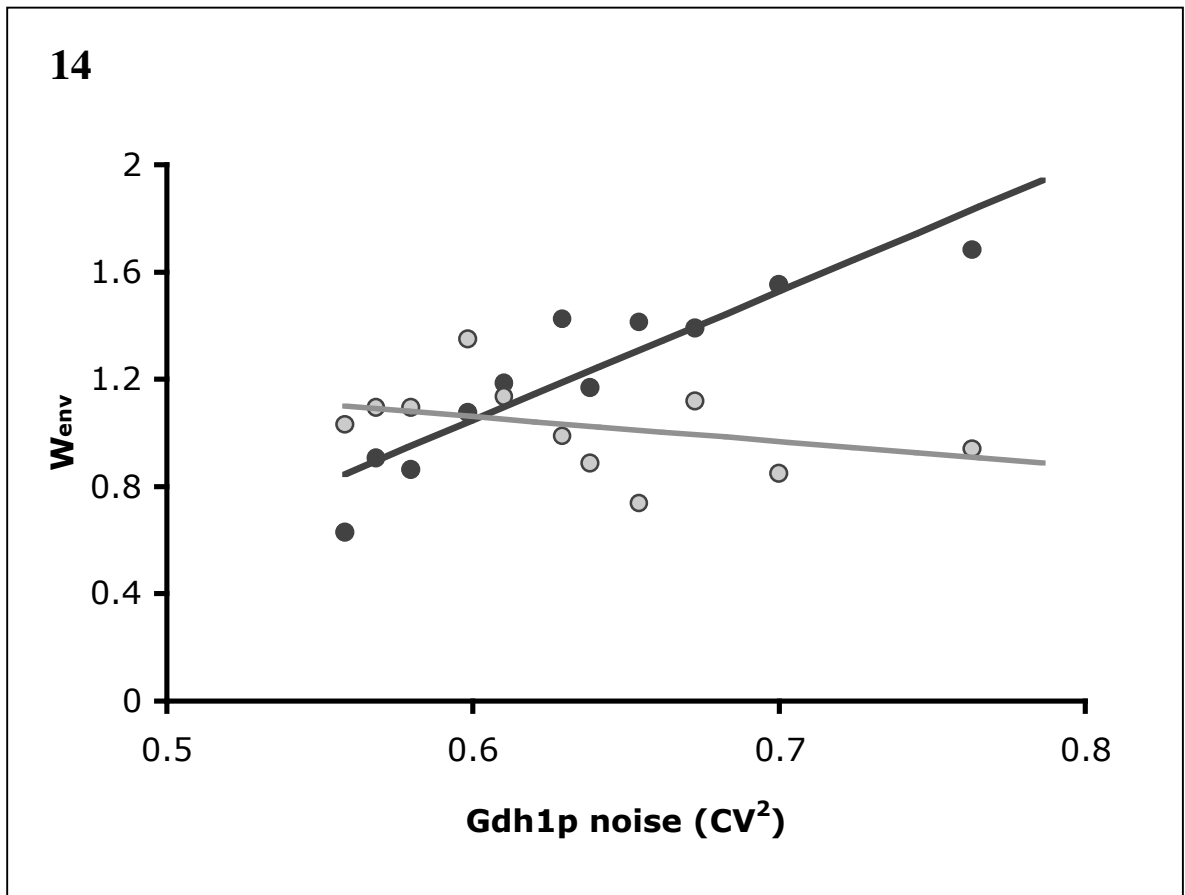
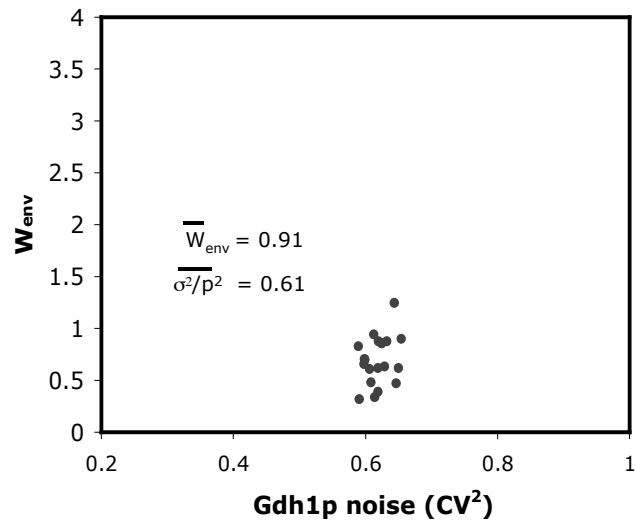
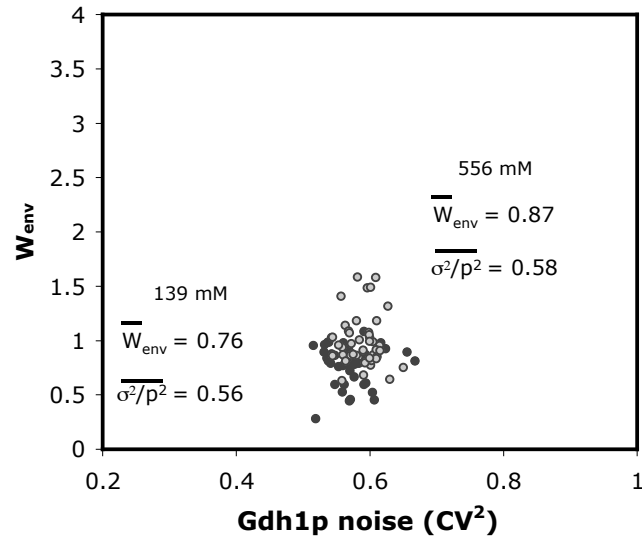


**Figure 14 Overexpression of Glt1p lowers  $W_{env}$  dependence on noise.**  $W_{env}$  as a function of Gdh1p noise in a set of *GDH1* promoter mutants transformed with a Glt1p overexpression plasmid (grey). This mutant promoter set transformed with an empty plasmid is shown for comparison (black). The trend of  $W_{env}$  with noise observed in the mutant set under wildtype Glt1p expression levels is diminished under Glt1p overexpression. The mean  $\pm$ s.d. from at least three independent experiments is shown.

15a



15b



15c

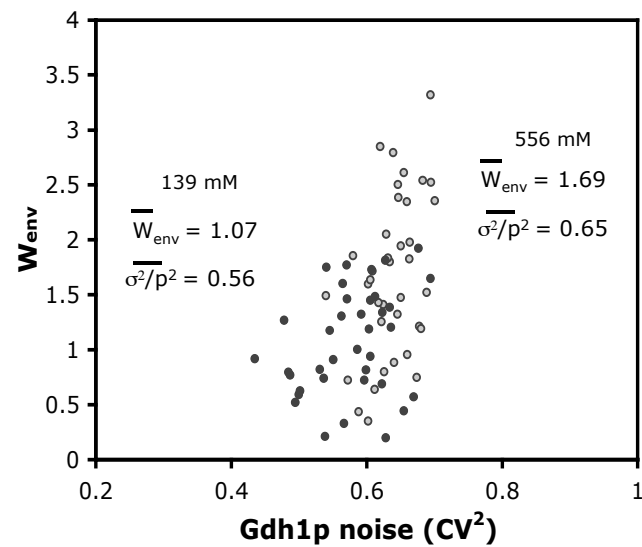


**Figure 15 Environmental selection pressure shapes Gdh1p noise in adapted populations. a,**  $W_{\text{env}}$  versus noise for the initial library ( $t = 0$ ). Mean  $W_{\text{env}}$  and Gdh1p noise values for the population are shown ( $n = 30$ ). **b,**  $W_{\text{env}}$  versus noise for the Day 3 population ( $\sim 36$  generations) from the 139 mM ammonia (grey,  $n = 48$ ) and 556 mM ammonia (black,  $n = 45$ ) selection conditions. **c,** Noise versus  $W_{\text{env}}$  for the Day 5 population ( $\sim 60$  generations,  $n = 48$  for both conditions). All errors are within 5% of the reported values.

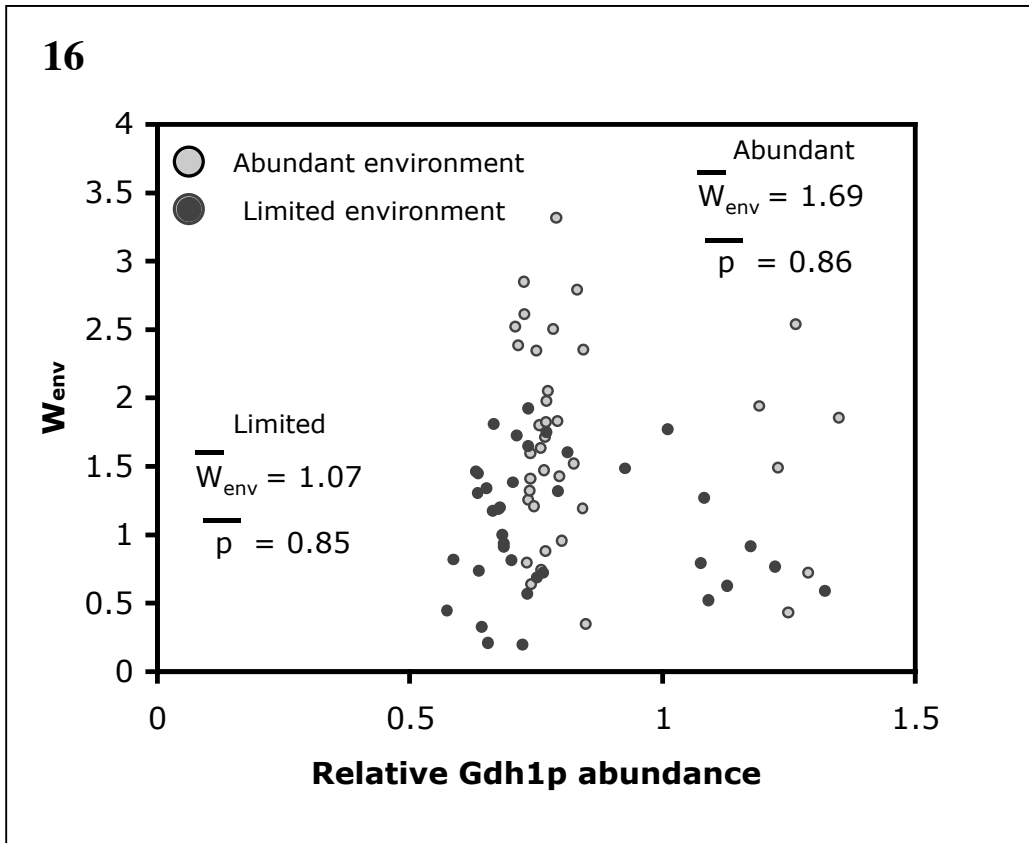


**Figure 16 Environmental selection pressure does not affect Gdh1p abundance.** Mean Gdh1p abundance versus  $W_{env}$  for the Day 5 adapted populations (~60 generations) selected in ammonia-abundant (grey) and ammonia-limited (black) conditions. The population-averaged Gdh1p abundance for individual clones from each environment is shown. Differences in average Gdh1p abundance for each population are not significant (mean Gdh1p = 0.86 relative to the parent strain for the abundant environment, mean Gdh1p = 0.86 relative to the parent strain for the limited environment,  $P = 0.72$ ), in contrast to the differences observed in average Gdh1p noise. Each point was measured in triplicate and error was within 5% of the reported value.

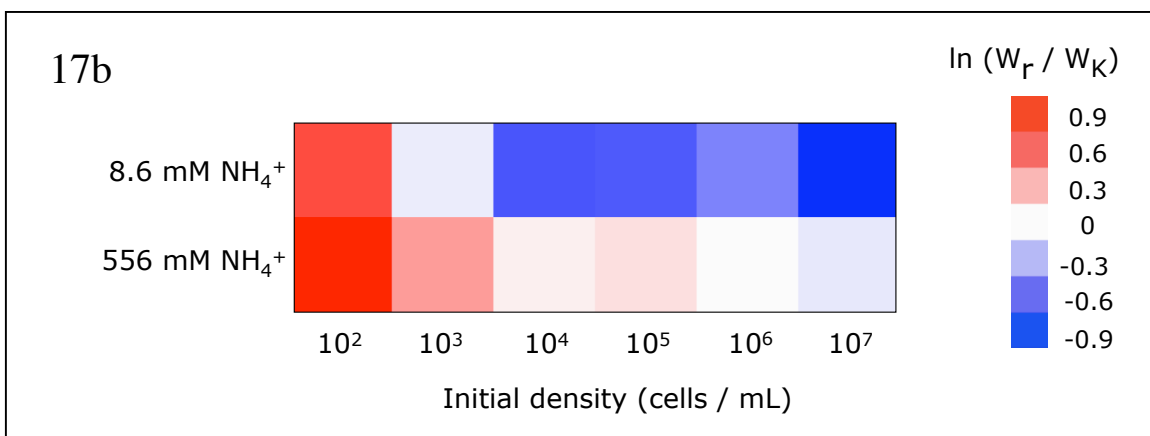
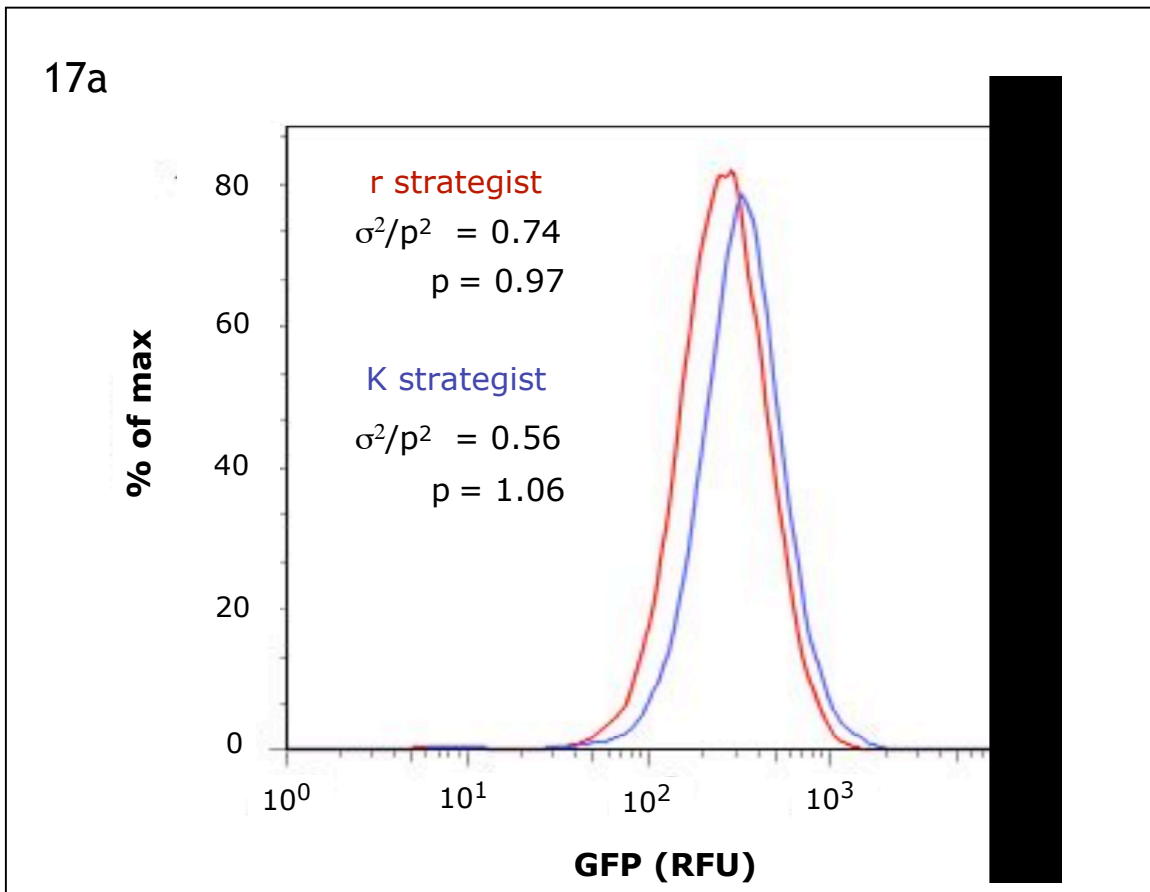


**Figure 17. a,** Representative histogram of Gdh1p expression in the r (red) and K (blue) strains. Abundance is reported relative to the parent strain. **b,** Density-dependent fitness for the r and K strains in poor and abundant ammonia environments. Fitness is reported as the natural log ratio of r strain fitness to K strain fitness and is represented as red and blue shading. Experiments were performed in triplicate and error is within 5% of the reported values.